

WATERFLOODING AND WATER-ALTERNATING-CO₂ INJECTION: EFFECT OF
INJECTED BRINE SALINITY

A Thesis

by

RAJA SUBRAMANIAN RAMANATHAN

Submitted to the Office of Graduate and Professional Studies of
Texas A&M University
in partial fulfillment of the requirements for the degree of

MASTER OF SCIENCE

Chair of Committee,	Hisham Nasr-El-Din
Committee Members,	David Schechter
	Mahmoud El-Halwagi
Head of Department,	A. Daniel Hill

December 2015

Major Subject: Petroleum Engineering

Copyright 2015 Raja Subramanian Ramanathan

ABSTRACT

Over the past fifty years, Improved Oil Recovery (IOR)/Enhanced Oil Recovery (EOR) technologies have been modified to include the effects of salinity of injected brine on oil recovery. Water-Alternating-Gas (WAG) is one such EOR process in the field. It improves the synergy of various individual mechanisms underlying EOR processes, such as ion exchange, wettability alteration, and mobility control. This process has matured over the years, but the alteration of the salinity of injected brine during WAG has not been extensively tested. This work investigates the effect of injected brine salinity during water-alternating-CO₂ injection and compares its performance with stand-alone brine injection, using 20 in. length outcrop Grey Berea sandstone cores. The water-alternating-CO₂ process was done under immiscible conditions. This work also studies the effect of aging of cores on oil recovery during the waterflooding process.

In the present work, six coreflood experiments were performed: four experiments before aging the cores and two experiments after aging the cores. The temperature was set at 149 °F (65 °C) for all the experiments. This work evaluated the oil recovery and pressure drop for each coreflood. The effect of salinity on rock wettability during waterflooding and water-alternating-CO₂ processes was studied using axisymmetric contact angle measurements.

The effect of salinity on the waterflooding process, as well as the water-alternating-CO₂ injection process, was observed throughout the coreflood experiments. Low-salinity brine yielded the highest recovery during the waterflooding process in aged

cores, and seawater brine yielded the highest recovery during the water-alternating-CO₂ injection process. Wettability alteration toward a more water-wet state improved the oil recovery during the low-salinity brine injection process. The lower solubility of CO₂ in seawater brine, compared to the solubility of CO₂ in low-salinity brine, resulted in higher oil recovery by seawater brine during the water-alternating-CO₂ injection process.

Fines migration was observed during the low-salinity brine-alternating-CO₂ injection process. Aging the cores improved the oil recovery during the waterflooding process. The salinity of brine affected the contact angle measurements of the Grey Berea sandstone rock. The rock was strongly water-wet in the presence of low-salinity brine. Seawater brine made the rock more oil-wet due to the ion binding nature of the divalent ions in seawater brine. The aging of the cores increased the contact angle of the rock, thereby making the rock more oil-wet. These findings provide a basis for optimizing the salinity of injected brine during the waterflooding and water-alternating-CO₂ injection.

DEDICATION

To my grandmother, parents and my brother

ACKNOWLEDGMENTS

I would like to thank my committee chair, Dr. Hisham Nasr-El-Din, for his continuous support and guidance throughout the course of this research. I would like also to thank Dr. David Schechter and Dr. Mahmoud El-Halwagi for serving as the committee members.

I would like to thank my friends, colleagues, and the department faculty and staff for making my time at Texas A&M University a great experience.

Finally, thanks to my parents and my brother for their encouragement.

NOMENCLATURE

IOR	Improved Oil Recovery
EOR	Enhanced Oil Recovery
WAG	Water-Alternating-Gas
USBM	U.S. Bureau of Mines
IFT	Interfacial Tension
DSA	Drop Shape Analyzer
ppm	Parts Per Million
XRD	X Ray Powder Diffraction
SEM	Scanning Electron Microscope
XRF	X Ray Fluorescence
HPHT	High Pressure-High Temperature
S_{wc}	Connate Water Saturation
CA	Contact Angle
OOIP	Original Oil In Place

TABLE OF CONTENTS

	Page
ABSTRACT	ii
DEDICATION	iv
ACKNOWLEDGMENTS.....	v
NOMENCLATURE.....	vi
TABLE OF CONTENTS	vii
LIST OF FIGURES.....	ix
LIST OF TABLES	xi
CHAPTER I INTRODUCTION	1
CHAPTER II LITERATURE REVIEW	6
CHAPTER III STATEMENT OF PURPOSE	14
CHAPTER IV OBJECTIVES	15
CHAPTER V MATERIALS	16
Rock Properties	16
Fluids.....	17
CHAPTER VI EXPERIMENTAL PROCEDURE.....	20
Components of the Drop Shape Analyzer.....	20
Preparation of Contact Angle Experiments.....	22
Contact Angle Experiments	24
Components of the Coreflood Apparatus.....	25
Preparation of Cores.....	28
Coreflood Experiments	29
CHAPTER VII RESULTS AND DISCUSSION.....	31
Effect of Salinity of Injected Brine on Contact Angle during Waterflooding Process.....	31
Effect of Salinity of Injected Brine on Contact Angle during Water- Alternating-CO ₂ Process	34
Effect of Salinity of Injected Brine on Oil Recovery during Waterflooding.....	36
Effect of Aging on Oil Recovery during Waterflooding.....	43

Effect of Salinity of Injected Brine on Oil Recovery during WAG.....	43
Waterflooding vs. WAG	51
CHAPTER VIII CONCLUSIONS.....	53
REFERENCES.....	55

LIST OF FIGURES

	Page
Fig. 1 — Waterflooding process	3
Fig. 2 — Water-Alternating-CO ₂ process	4
Fig. 3 — A schematic diagram of the drop shape analyzer apparatus.	21
Fig. 4 — Analysis of the crude oil droplet	24
Fig. 5 — A schematic diagram of the coreflood apparatus.	27
Fig. 6 — Effect of temperature on the equilibrium contact angle of unaged Grey Berea sandstone rock at 500 psi during waterflooding process.	33
Fig. 7 — Effect of temperature on the equilibrium contact angle of aged Grey Berea sandstone rock at 500 psi during waterflooding process.	33
Fig. 8 — Effect of time on the dynamic contact angle of unaged Grey Berea sandstone rock at 500 psi and 149 °F during water-alternating-CO ₂ process.	36
Fig. 9 — Oil recovery and pressure drop across the core for experiment A-1 at 149 °F. The injection was performed with NaCl brine (5,000 ppm) using injection rates of 0.5, 1, 2, and 4 ml/min. The vertical dashed lines separate the different injected brine stages.	38
Fig. 10 — Oil recovery and pressure drop across the core for experiment A-2 at 149 °F. The injection was performed with seawater brine using injection rates of 0.5, 1, 2, and 4 ml/min. The vertical dashed lines separate the different injected brine stages.	39
Fig. 11 — Oil recovery and pressure drop across the core for experiment A-3 at 149 °F. The injection was performed with NaCl brine (5,000 ppm) using injection rates of 0.5, 1, 2, and 4 ml/min. The vertical dashed lines separate the different injected brine stages.	41
Fig. 12 — Oil recovery and pressure drop across the core for experiment A-4 at 149 °F. The injection was performed with seawater brine using injection rates of 0.5, 1, 2, and 4 ml/min. The vertical dashed lines separate the different injected brine stages.	42

Fig. 13 — Oil recovery and pressure drop across the core for experiment A-5 at 149 °F. The injection was performed with low-salinity-brine-alternating-CO ₂ . The vertical dashed lines separate the different injection stages.	46
Fig. 14 — Emulsion formation as a result of fines migration in Experiment A-5.....	48
Fig. 15 — Oil recovery and pressure drop across the core for experiment A-6 at 149 °F. The injection was performed with seawater-brine-alternating-CO ₂ . The vertical dashed lines separate the different injection stages.	49
Fig. 16 — Comparison of oil recovery between different processes on Grey Berea sandstone at T = 149°F.	52

LIST OF TABLES

	Page
Table 1 — Petrophysical properties of the used Grey Berea sandstone cores.....	16
Table 2 — Mineralogy of Grey Berea sandstone core.....	17
Table 3 — Composition of prepared brines.....	18
Table 4 — Density of prepared brines at T= 149 °F and P= 14.7 psi.....	18
Table 5 — Equilibrium contact angle images of Grey Berea-brine-oil-nitrogen system at 149 °F.....	34
Table 6 — Equilibrium contact angle images of Grey Berea-brine-oil-CO ₂ system at 149 °F.....	35
Table 7 — Summary of coreflood experiment (A-1) for unaged Grey Berea sandstone at T = 149 °F.....	38
Table 8 — Summary of coreflood experiment (A-2) for unaged Grey Berea sandstone at T = 149 °F.....	39
Table 9 — Summary of coreflood experiment (A-3) for aged Grey Berea sandstone at T = 149 °F.....	41
Table 10 — Summary of coreflood experiment (A-4) for aged Grey Berea sandstone at T = 149 °F.....	42
Table 11 — Summary of coreflood experiment (A-5) for unaged Grey Berea sandstone at T = 149 °F.....	46
Table 12 — Summary of coreflood experiment (A-6) for unaged Grey Berea sandstone at T = 149 °F.....	50

CHAPTER I
INTRODUCTION

Fossil fuel is still the biggest source of energy known to mankind. It constitutes about eighty percent of the energy consumption globally. The world demand for petroleum is on a constant rise, and it is projected to increase to 6,301 million tons of oil equivalent (MTOE) in 2030. Also, it is becoming increasingly difficult to discover new oilfields, and companies are focused on recovering the maximum amount of oil from their existing oilfields. Unfortunately, two-thirds of the oil in the reservoirs cannot be produced economically due to the physics of fluid flow. To meet the global demand, it is believed that IOR/EOR technologies will play a key role in the years to come. These methods are applied to recover the additional oil after the primary depletion process, where the oil is recovered through the natural drive of the reservoir. IOR/EOR methods improve the recovery factor of oil to about seventy percent. Waterflooding and Water-Alternating-Gas (WAG) are two widely used injection strategies that improve the productivity of a reservoir by generating an energy drive that pushes the oil towards the production wells.

The effectiveness of an IOR/EOR technology depends on the capillary number and mobility ratio. The capillary number is the measure of the relative effect of viscous forces against surface tension acting across an interface between two immiscible liquids. It is represented by the following formula:

$$N_c = \frac{\vartheta\mu}{\sigma\cos\theta} \dots\dots\dots (1)$$

Where ϑ is the darcy's velocity, μ is the viscosity of the displacing fluid, σ is the interfacial tension between the displaced and displacing fluid, and θ is the contact angle between the oil-water interface and rock surface. If the capillary number is much greater than one, viscous force dominates the interfacial tension and vice versa if the capillary number is much less than one. At a capillary number much less than one, capillary forces dominate the flow in porous media. The mobility ratio is defined as the mobility of the displacing phase divided by the mobility of the displaced phase. It is given by the following formula:

$$M = \frac{\lambda_{displacing}}{\lambda_{displaced}} \dots\dots\dots (2)$$

If $M < 1$, the displacement is stable, and there is a sharp shock front, whereas if $M > 1$, there is channeling of displacing fluid. As a result there is some bypassing of residual oil. $M = 1$ denotes piston-like displacement and is the most favored mobility ratio for oil recovery processes. The oil recovery factor is mathematically represented by the relationship between the microscopic and macroscopic recovery efficiencies. It is given by the following formula:

$$R_f = E_v \times E_h \times E_m \dots\dots\dots (3)$$

Where E_v and E_h represent the macroscopic vertical and horizontal sweep efficiency, and E_m indicates the microscopic sweep efficiency. The macroscopic efficiency is determined by the fluid density difference and the rock heterogeneity, whereas the microscopic efficiency depends on the interactions involving the interfacial

forces like interfacial tension and contact angles. Waterflooding and water-alternating-gas technology uses these fundamental concepts to boost the recovery factor and obtain both technical and economic success.

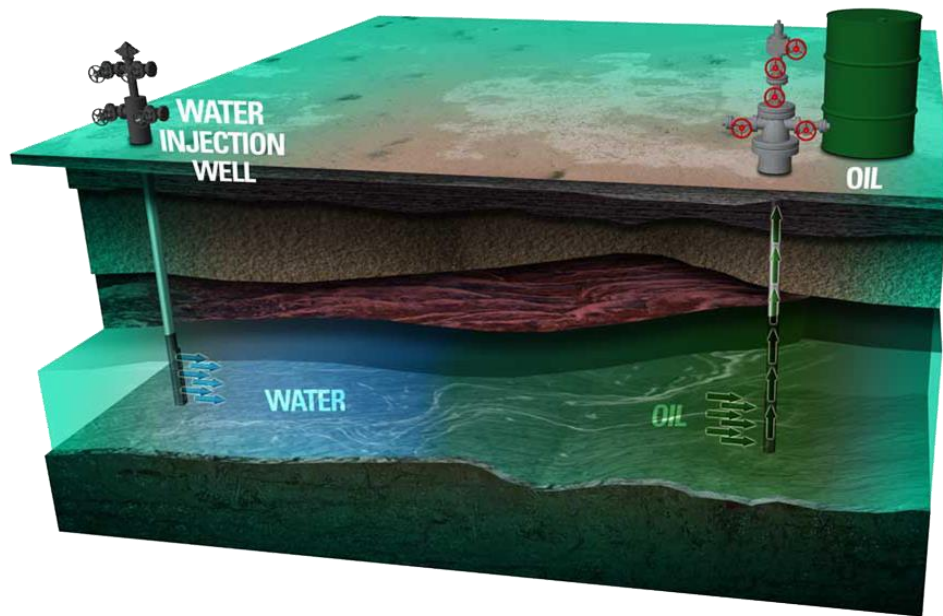


Fig. 1 — Waterflooding process.

Waterflooding was found as an accident in the Bradford field of Pennsylvania during the 1890s, when fresh water started entering the producing zones and increased the production of oil. This practice rapidly expanded after 1921, and different water injection scenarios were implemented in the field. Waterflooding is termed as secondary recovery because it is executed immediately after primary production. **Fig. 1** represents a conventional waterflooding process. During the primary production of crude oil, the reservoir pressure dissipates continuously, and the natural drive mechanism of the reservoir is not sufficient to produce oil at an economic rate. Also, more than eighty percent of the oil gets left behind in the reservoir. Waterflooding is then employed to

improve the oil production rate. It does so by increasing the reservoir pressure to its initial level. Most reservoirs in the world employ waterflooding to enhance the production of oil, mainly because of its simplicity and reliability. Before 1970, the injected brine composition was chosen to be compatible with the formation brine to prevent formation damage. The idea of low-salinity brine injection was implemented during the 1970s in the field after reports of improved oil recovery due to the change in brine composition.

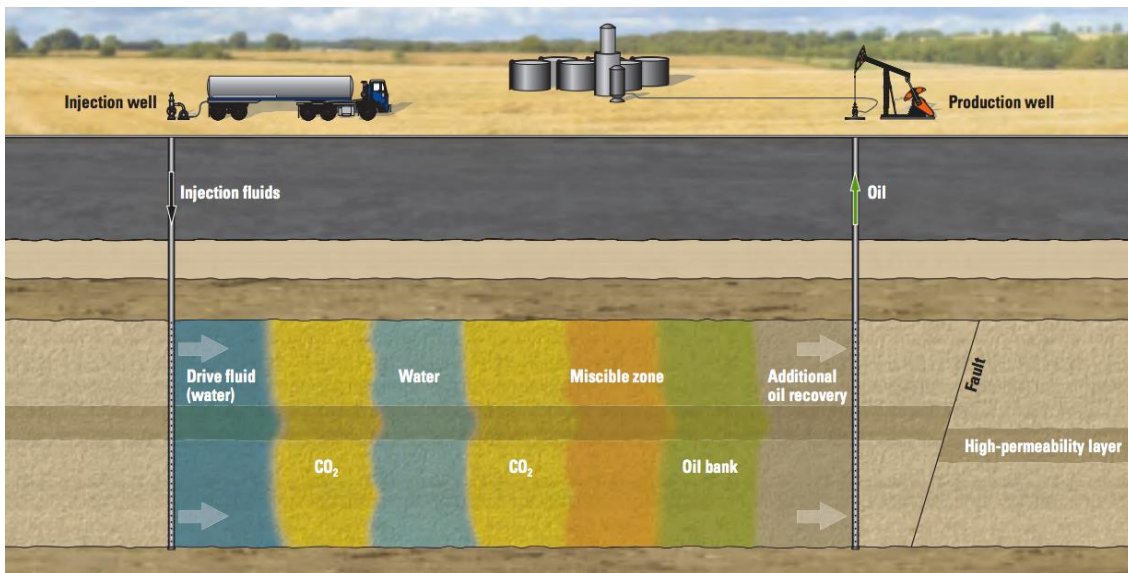


Fig. 2 — Water-Alternating-CO₂ process

Fig. 2 demonstrates a conventional WAG process. WAG injection is a form of tertiary recovery in which alternate slugs of water and gas are injected into the reservoir. WAG takes advantage of the decreased mobility of the water-gas mixture and can recover the bypassed oil in the reservoir. In most cases, forty percent of the original oil in place still remains to be recovered after secondary recovery. WAG is then executed to recover the remaining oil in place. CO₂ is the most commonly used gas during WAG because of its economic feasibility, its ability to swell oil, and its environmental benefits. This

technique of injection was an evolutionary step in the technical and economical implementation of CO₂ as a tertiary recovery process. The CO₂ pipeline system is well developed, and the availability of CO₂ at a very cheap price of \$1–2 per thousand cubic feet makes it a very attractive option to be used as an EOR technology in the United States of America (USA). As per the 2014 National Energy Technology Laboratory (NETL) report, there are 113 CO₂ EOR projects in the USA, and they inject a cumulative 3.1 billion cubic feet per day of CO₂ to recover 282,000 barrels of crude oil per day from multiple locations. By 2020, the number of projects is projected to increase to 124 that will recover 615,000 barrels of crude oil per day. CO₂ WAG has various forms: miscible WAG, immiscible WAG, simultaneous WAG, and hybrid WAG. Immiscible WAG is a process where the gas is not fully miscible with the oil. The optimum utilization of the injected gas determines the success of the WAG project. The factors that influence oil recovery during WAG injection are: heterogeneity, wettability, fluid properties, miscibility conditions, injection techniques, WAG parameters, physical dispersion, and flow geometry.

CHAPTER II

LITERATURE REVIEW

Recent studies in IOR methods have changed the most fundamental piece in any waterflooding process: injection brine composition. The chemistry of injected water largely determines the oil recovery from several improved such methods. The physicochemical perspective on water/oil interactions is very important in designing and optimizing such processes. Early research work in this field started during the 1990's with researchers modifying the salinity of injected brine in all types of rocks. Buckley et al. (1989) showed that the composition of injected brine can have a dominant effect on the wetting behavior of crude oil. They observed that the adhesion of crude oil on flat glass surfaces depends on the brine composition. They also formed stable emulsions of crude oil in brine and noticed a change in electrophoretic mobility with a change in brine composition.

Jadhunandan (1990) studied the effect of brine composition on wettability and oil recovery. He observed that the oil recovery was maximum for weakly water-wet/mixed wet systems rather than for strongly water-wet/oil-wet systems. The work used three inch Berea sandstone cores and conducted the tests at 300 psi. Two crude oils, Moutray and ST-86, were used to observe the effect of crude oil type on wettability of the system. Moutray showed sensitivities to the wettability when different brine compositions were used, whereas ST-86 was found to be insensitive. The author also noted that the aging temperature played a significant role in determining the wettability of the system.

Jadhunandan and Morrow (1995) investigated the effect of aging temperature on the wettability of sandstone rock and conducted waterflood tests using different crude oils and refined oils. The sensitivity of wettability to the brine composition decreased with an increase in aging temperature for Moutray crude oil. ST-86 showed less overall change in the wettability with the change in aging temperature. The wettability index was consistently lower for brines with a higher calcium content.

Morrow et al. (1998) studied the effect of individual cations on waterflood recovery. They did contact angle measurements on pure quartz plates. They observed more water-wetness in the presence of monovalent ions rather than divalent ions. Adsorption by ion binding was said to be the likely cause of this effect.

Several field tests have also been conducted based on low-salinity brine injection. Webb et al. (2004) tested this technology in an Alaskan sandstone reservoir. They conducted a log-inject-log field test to ensure low flow rates and minimal cross flow. The results were in agreement to the previously tested coreflood studies and showed a 25–35% reduction in the residual oil saturation when the reservoir was flooded with low-salinity brine. Their study used a brine containing 3,932 mg/kg chloride content.

Lager et al. (2008) conducted a study on the mechanism of low-salinity waterflood using 3” long core plug samples from sandstone oil reservoirs. They concluded that cation exchange between the injected brine and the rock was the primary mechanism of improved oil recovery during low-salinity waterflooding.

Even though there has been considerable success in the past by tailoring the brine composition during waterflooding, the mechanism of recovery is still debated. Authors

have cited wettability alteration by adsorption of cations on the rock's surface (Tang and Morrow 1999), in situ surfactant generation (McGuire et al. 2005), multicomponent ion exchange (Lager et al. 2008), expansion of the electrical double layer (Ligthelm et al. 2009; Nasralla et al. 2013), and microdispersion formation (Sohrabi et al. 2015) as the possible mechanisms of oil recovery by low-salinity waterflooding.

Oil recovery is highly dependent on the fluid-fluid and fluid-rock interactions (Chattopadhyay et al. 2002). Centrifuge coreflow tests were conducted using Berea sandstone and Texas Cream limestone. When crude oils were used, differences in the wetting phase capillary desaturation curves were found during primary and secondary drainage. However, this trend was not observed when decane was used as the oil phase.

When CO₂ is introduced into the reservoir, various phenomena take place, which depend on the properties of the rock and reservoir fluids. The use of CO₂ in EOR applications started back in 1952 by Whorton and Brownscombe (Stalkup 1978). They filed a patent which involved the injection of CO₂ into an oil reservoir to recover more oil than was previously recoverable using the known methods of production.

CO₂ EOR has since become an area of focus for many industrial and research purposes (Johnson et al. 1952; Caudle and Dyes 1958; Holm 1959; Beeson and Orloff 1959; Graue and Zana 1981; Orr Jr. et al. 1982; Holm 1987; Thomas and Monger-McClure 1991; Martin and Taber 1992; Dong et al. 2000; Manrique et al., 2007; Ghedan 2009; Alvarado and Manrique 2010; Chen et al. 2010; Sinisha 2012; Sahin et al. 2012; Kamali et al. 2015). CO₂ EOR was in a decline from 1985 to 2005, but it has evolved during the last decade. WAG has always been the preferred method of gas EOR in the industry

because of its synergy of various EOR mechanisms such as ion exchange, wettability alteration, and mobility control. It also has applications in underground CO₂ sequestration. Research in the area of WAG has advanced to using foams, gels, steam, and CO₂ thickeners to mitigate the gravity override/viscous fingering effects (Woods et al. 1986; McClain et al 1996; Hild and Wackowski 1999; Enick et al. 2012; Ali and Schechter 2013). Even though these processes have yielded remarkable results, the complexity of the WAG process has increased through these modifications.

Arguably, the simplest modification of a typical WAG process involves changing the ionic composition of brine. Changing the salinity of injected brine during the WAG process has received limited attention in literature. Kulkarni and Rao (2005) tested the effect of salinity on the tertiary WAG process by comparing the oil recovery of 5 wt% NaCl to 0.9 wt% multivalent ions on Berea sandstone and observed a decrease in oil recovery with a decrease in salinity. They demonstrated the effect of salinity of injected brine by conducting immiscible and miscible WAG floods with one foot long Berea sandstone cores and two different kinds of brine. n-Decane was the oleic phase, and pure CO₂ was used as the gas phase for all of the studies. There was a 6% increase in oil recovery when 0.9 wt% multivalent ions were used as the brine phase during immiscible WAG injection.

Al-Netaifi (2008) conducted CO₂ WAG corefloods with two different brine compositions and observed similar oil recoveries in both and a faster recovery by the higher salinity brine.

Aleidan and Mamora (2010) conducted secondary miscible corefloods in heterogeneous carbonate cores. They used 0, 6, and 20 wt% brines to study the effect of salinity on carbonate cores. Lowering the brine salinity yielded higher recovery factor during water-alternating-CO₂ floods. It was attributed to the better displacement efficiency offered by the lower salinity brine-CO₂ mixture.

Jiang et al (2010) performed tertiary miscible CO₂ WAG corefloods on Berea sandstones and concluded that WAG recovery decreased at lower salinities because of a higher CO₂ solubility in brine.

Zolfaghari et al. (2013) conducted immiscible WAG corefloods with Berea sandstone cores and showed a higher ultimate oil recovery of 18% for low-salinity WAG compared to a higher salinity WAG. They used three inch cores, multivalent brines, and 28° API filtered heavy crude oil for their study.

Dang et al. (2013) have conducted a numerical simulation work on miscible CO₂ WAG process and showed an increase of oil recovery by 9% OOIP. They have extended this study to field scale as well (Dang et al. 2014). CO₂ LSWAG solves the problem of late production problem that is usually encountered during conventional WAG.

Eighty percent of the oil reservoirs in the world are said to be suitable for CO₂ injection. Project success is strongly dependent on the interfacial interactions, such as interfacial tension and wettability. The ability of the fluid to adhere to a rock's surface is determined by the rock's wettability (Yang et al. 2008). The wettability of a rock is very crucial in determining the fluid behavior and fluid distribution in the rock. Wettability of a rock is determined based on the following parameters: oil composition, surface

chemistry of the rock, temperature, pressure, and contact time (Wang and Gupta 1995; Jadhunandan and Morrow 1995). Wang and Gupta (1995) measured the contact angle and the interfacial tension of two different crude oil-brine-quartz/calcite and mineral oil-distilled water systems for different ranges of temperatures and pressures. They observed an increase in contact angle with increasing pressure and temperature for the sandstone system and the opposite for the carbonate system. The IFT increased with pressure for all of the systems studied.

Over the last fifty years, there has been a lot of research in the area of wettability determination and its relation to oil recovery with contrasting results (Donaldson et al. 1969; Anderson 1986; Morrow 1990; Cuiec 1991; Morrow et al. 1998; Zhou et al. 2000; Chattopadhyay et al. 2002; Nasralla and Nasr-El-Din 2014). Some authors have reported that maximum oil recovery was obtained by strongly water-wet conditions, while others have reported mixed wet/weakly water-wet conditions to be the reason for maximum oil recovery. There is a lack of consensus on the relationship between the wettability of the rock and oil recovery (Agbalaka et al. 2008). The Amott method, the US Bureau of Mines (USBM) method, and the contact angle method are the quantitative approaches available to determine wettability. The Amott and USBM method are used to measure the average wettability of a reservoir core. The contact angle method is used to measure the wettability of a specific solid surface. Many parameters influence the contact angle method, such as surface roughness, viscous effects, contact line fluctuations, and vibrations, but it is the easiest experiment to conduct and can be applied at high temperatures and pressures (Ameri et al. 2013). A rock is said to be water-wet, mixed-wet, or oil-wet if the advancing

contact angle of water on a solid surface is in the range of 0-75°, 75-105° or 105-180°, respectively (Anderson 1986; Alotaibi et al. 2011). The ionic concentration of the brine has been proven to have a significant effect on the wettability of the rock during waterflooding processes (Morrow et al. 1998; Yildiz et al. 1999; Chattopadhyay et al. 2002; Alotaibi et al. 2011; Nasralla and Nasr-El-Din 2014; Shehata and Nasr-El-Din 2015).

Yildiz et al. (1999) used spontaneous imbibition experiments to determine the effect of ionic concentration on the wettability of the rock. Brine composition had different effects on the waterflood recovery of Moutray and A'92 crude oil, but depressed imbibition led to a higher waterflood recovery for all the cases.

Alotaibi et al. (2011) indicated that low-salinity water expanded the double-layer thickness and provided an opportunity for wettability alteration. Clay content was observed to be an important factor in wettability alteration of sandstone rocks.

Shehata and Nasr-El-Din (2015) conducted zeta potential experiments between four different sandstone rock types and five different brines. They found that monovalent cations increase the absolute values of zeta potential more effectively than divalent ions. Carbonate rocks showed a different trend of zeta potential compared to the sandstone rocks.

CO₂ has been widely known to affect the wettability of the rock. Yang et al. (2008) measured the dynamic and equilibrium contact angles of a rock/brine/oil/CO₂ system at different pressures and temperatures. They correlated the obtained wettability alteration to the oil recovery during tertiary injection processes. The equilibrium contact angles

through the crude oil phase increased as the pressure increased but decreased with an increase in temperature. They concluded that wettability alteration occurred when CO₂ was injected into an oil reservoir and would hence affect the oil recovery.

Ameri et al. (2013) compared the dependence of pressure on water-wet and oil-wet systems. They studied the effect of the pressure on the contact angle of a rock under a certain wetting condition. For a partially water-wet surface, the contact angle did not change with pressure, whereas for an oil-wet surface, higher pressures resulted in higher contact angles. CO₂ was noted as the nonwetting phase in the studied pressure and salinity range.

Agbalaka et al. (2008) reviewed the gas injection modes and its dependence on the wettability of the rock. They noted that the gas flood recovery during secondary mode was best for mixed wet/water-wet systems. The authors have stated that the oil recovery was not only dependent on the wettability of the rock, but it was also dependent on other reservoir rock and fluid properties.

Jaeger et al. (2010) conducted contact angle and interfacial tension measurements using carbon dioxide. They observed reduction in IFT and changes in contact angle over time when CO₂ was introduced in the system. They noted that CO₂ has a significant effect on the phase behavior and the interfacial tension. In presence of CO₂, the IFT significantly decreased for all the tested temperatures.

CHAPTER III

STATEMENT OF PURPOSE

Detailed literature studies have been made in the area of IOR/EOR methods to enhance the oil recovery by reducing the residual oil saturation. Kulkarni and Rao (2005) first tested the salinity of injected brine on the oil recovery due to WAG. They used n-decane as the oleic phase for their experiments. Al-Netaifi (2008) conducted two miscible WAG corefloods with two different brines and n-decane as the oil phase. Aleidan and Mamora (2010) observed the effect of salinity of injected brine during WAG injection on oil recovery in carbonate cores. Jiang et al. (2010) performed tertiary miscible CO₂ WAG floods on 10.5 inch long Berea sandstones and observed the effect of divalent ions on the oil recovery. Zolfaghari et al. (2013) conducted immiscible WAG corefloods to recover heavy oil from three inch long Berea sandstone cores.

There are gaps in literature that needs to be addressed. The effect of brine salinity on immiscible CO₂ WAG has received limited attention, and systematic experimental work is required to understand this phenomena. This work will investigate the effect of salinity of injected brine on the performance of the immiscible water-alternating-CO₂ injection and waterflooding process. It will use 20 inch Grey Berea sandstone cores and 41 °API crude oil. The effect of salinity of the injected brine on the wettability of the rock will be studied and correlated with the coreflood experiments. This work will also study the effect of aging of cores on oil recovery during the waterflooding and WAG injection process. The mechanism of oil recovery in each case will be evaluated and discussed.

CHAPTER IV

OBJECTIVES

To complete this work, eight coreflood experiments will be performed: four experiments before aging the cores and four experiments after aging the cores. The experiments will be done at 149 °F (65 °C). Both the waterflooding and water-alternating-CO₂ injection will be done in the secondary mode of recovery, and the oil recovery will begin from the initial oil saturation of the core. The WAG experiments will be performed at immiscible conditions. This work will evaluate the oil recovery and pressure drop for each coreflood. The effect of salinity of injected brine and aging of core on the rock wettability during the waterflooding and water-alternating-CO₂ injection processes will be studied using axisymmetric contact angle measurements. The results from the contact angle measurements will be correlated to the coreflood experimental results.

CHAPTER V

MATERIALS

Rock Properties

A total of six cylindrical cores were drilled from a homogeneous outcrop Grey Berea sandstone block. Each core was 1.5 in. in diameter and 20 in. in length. Permeability anisotropy was maintained by drilling the cores along one direction. A coreflood apparatus was used to measure the porosity and permeability of each core. The petrophysical properties of each core sample are given in **Table 1**.

Core ID	RSR 5	RSR 8	RSR 11	RSR 17	RSR 20	RSR 22
Length (in.)	20	20	20	20	20	20
Porosity (vol%)	17.9	17.6	18.7	18.8	17.7	19.1
Brine permeability (md)	75.8	79.2	77.6	62.1	73.2	77.7
Connate water saturation (%)	44	44	40	37.5	42	43
Initial oil saturation (%)	56	56	60	62.5	58	57

Table 1 — Petrophysical properties of the used Grey Berea sandstone cores.

The Grey Berea sandstone rock was characterized using x-ray diffraction (XRD), scanning electron microscope (SEM), and x-ray fluorescence (XRF). The results of the XRD and SEM tests were analyzed for the mineralogy composition of the rock and presented in **Table 2**. Grey Berea sandstone rock has a relatively high percentage of kaolinite compared to other outcrop cores in the literature including Buff Berea, Parker, and Bandera.

Mineral	Concentration (wt%)
Quartz	87
Kaolinite	6
Albite	3
Illite	2
Calcite	2

Table 2 — Mineralogy of Grey Berea sandstone core

Fluids

Formation brine with a 174,156 ppm salt concentration was used as a connate brine for all of the cores. Additionally, the coreflood studies used seawater brine with a salinity of 54,680 ppm and low-salinity brine with 5,000 ppm NaCl. To prepare the brines, different predetermined salts were dissolved in deionized water with a resistivity of 18.2 ohms-m. **Table 3** presents the composition of the brines. The densities of all of the brines at 149 °F and atmospheric pressure are shown in **Table 4**. The density was determined using a density meter.

Salt	Formation Brine (mg/l)	Seawater Brine (mg/l)	Low-salinity Brine (mg/l)
NaCl	137735.01	38386.284	5000
CaCl ₂ ·2H ₂ O	38881.86	2435.618	-
MgCl ₂ ·6H ₂ O	13463.63	19058.138	-
Na ₂ SO ₄	547.08	5263.816	-
NaHCO ₃	242.32	265.722	-
Total dissolved solids	174156	54680	5000

Table 3 — Composition of prepared brines.

Brine	Density (g/cm ³)
Formation water (174,156 ppm)	1.15
Seawater (54,680 ppm)	1.01
NaCl (5,000 ppm)	0.95

Table 4 — Density of prepared brines at T= 149 °F and P= 14.7 psi.

A 41 °API dead crude oil sample was used for all experiments. This crude oil was centrifuged for five minutes at 5,000 rpm to make sure it is free from suspended solids and aqueous phase. To make sure that there was no plugging or emulsion problems, the crude oil was filtrated through a sandstone core.

Carbon dioxide with 99.8% purity (impurities were mainly water vapor and nitrogen) and nitrogen of 99.9% purity were used for all experiments. Carbon dioxide was used in the gaseous phase for all the experiments.

CHAPTER VI

EXPERIMENTAL PROCEDURE

Components of the Drop Shape Analyzer

The contact angle measurements were done using a DSA (**Fig. 3**). The DSA consisted of the following components:

1. High-pressure high-temperature (HPHT) view chamber. (Eurotechnica GmbH, Germany, Pmax = 10,000 psi, Tmax = 392 °F, stainless steel material 1.4436)
2. A substrate holder that held the rectangular rock tile above the capillary needle.
3. An oil accumulator that held the oil, which was injected into the chamber through the capillary needle.
4. Temperature controller (Hillesheim HT 40, Germany, control range: 32-212°F) that controlled the temperature inside the chamber.
5. A thermocouple of type K that was inserted directly into the view chamber to monitor its temperature. The thermocouple had an accuracy of 0.1K.
6. A compressed nitrogen or a compressed CO₂ cylinder, through which pressure was applied to the chamber. The pressure inside the chamber was monitored using a pressure transducer (Eurotechnica, Germany).
7. An image data acquisition system that took high resolution images of the oil droplet.
8. A computer having the drop shape analysis software. The image from the camera was sent to the computer, which helped in analyzing the contact angle.
9. Vents and drains, used to eject the fluids from the cell.

10. A light source that was used to illuminate the chamber.

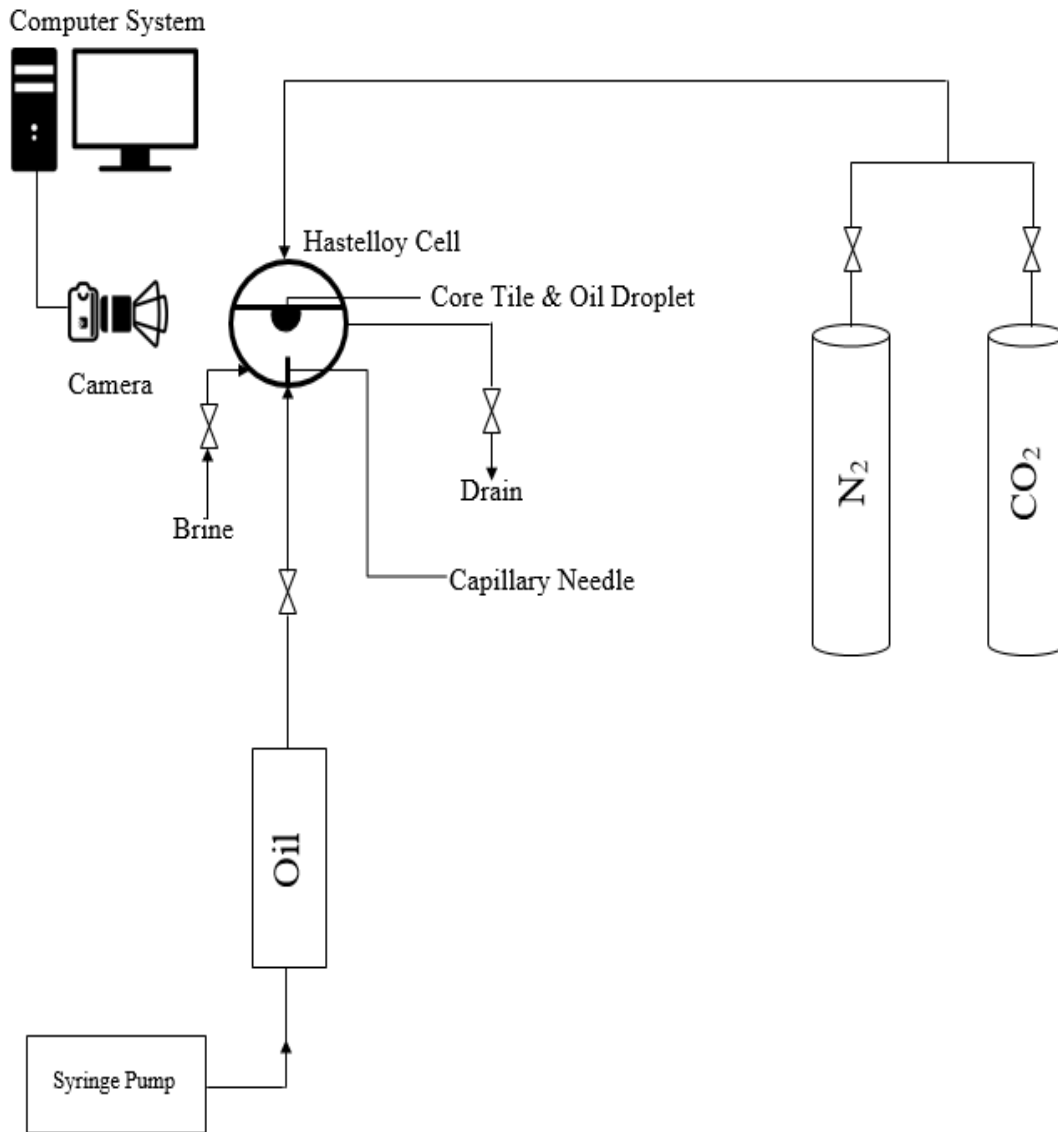


Fig. 3 — A schematic diagram of the drop shape analyzer apparatus.

Preparation of Contact Angle Experiments

In all of the experiments, a rectangular core tile was used as the rock substrate, and it was prepared using the following procedure:

1. The substrate was cut from a core plug and had the dimensions of 1.57 cm x 1.83 cm x 0.64 cm.
2. The substrate was then polished on both lateral sides using sandpaper of sizes 400 - mesh and 200 - mesh. This was done to minimize the contact angle hysteresis caused by surface roughness. The contact angle method of measuring wettability requires the solid surface to be smooth and homogeneous.
3. After polishing, the substrate was kept in a glass container containing formation brine for a period of one day.
4. The container was then subjected to vacuum pressure for 4 hours. This was done to remove the air pockets inside the substrate and ensure complete saturation.
5. The vacuum was then removed, and the substrates soaked in the formation brine for at least two days to ensure removal of contaminants and surface charges induced by polishing.
6. The substrate was removed from the formation brine and prepared for oil saturation. The substrate was placed in crude oil and centrifuged at 3,000 rpm for 30 minutes. The substrate was recentrifuged again at the same conditions after 30 minutes of waiting time. This ensured the substrates achieved connate water saturation (S_{wc}).

7. This substrate was used in the contact angle experiments for unaged cores. To age the substrates, it was kept in a glass container and placed inside an oven. The temperature of the oven was set at 149 °F, and the substrates were aged for 30 days.

Before the start of the experiment, all of the equipment flow lines were cleaned using toluene and deionized water, to ensure no presence of impurities. The substrate was then loaded into a substrate holder and placed in the HPHT chamber. The substrate was levelled horizontally before the chamber was closed using the viewing windows. It was properly locked in place to avoid any leakages during the experiment. The brine was then introduced into the chamber. The chamber was completely filled with brine and nitrogen/CO₂ was introduced to the chamber to act as a pressurizing medium. The temperature of the chamber was then changed using the temperature controller. The camera was placed in front of the chamber and was adjusted to focus on the rock substrate. A captive drop of crude oil was then injected through the capillary needle onto the surface of the substrate using an accumulator and a syringe pump. The drop was injected into the cell at a pressure 100 psi greater than the pressure inside the cell. The drop needs to be axisymmetric for these measurements. The image data acquisition system was used to take an image and it was analyzed using the computer. The drop shape analysis software in the computer determined the angles between the baseline and the tangent at the drop boundary (**Fig. 4**). All of the experiments conducted in this study measured the dynamic contact angle between the oil and the rock substrate. The advancing contact angle was measured through the brine phase, and therefore, rocks with $CA < 75^\circ$ were termed as water-wet,

rocks with CA between 75° and 105° were termed as mixed-wet, and rocks with $CA > 105^\circ$ were termed as oil-wet. After the experiment was completed, the temperature controller was switched off, and the cell was evacuated of the brine and nitrogen/ CO_2 through the discharge valve. The substrate holder was then removed from the cell after opening the glass windows. The cell was thoroughly cleaned using toluene and deionized water.

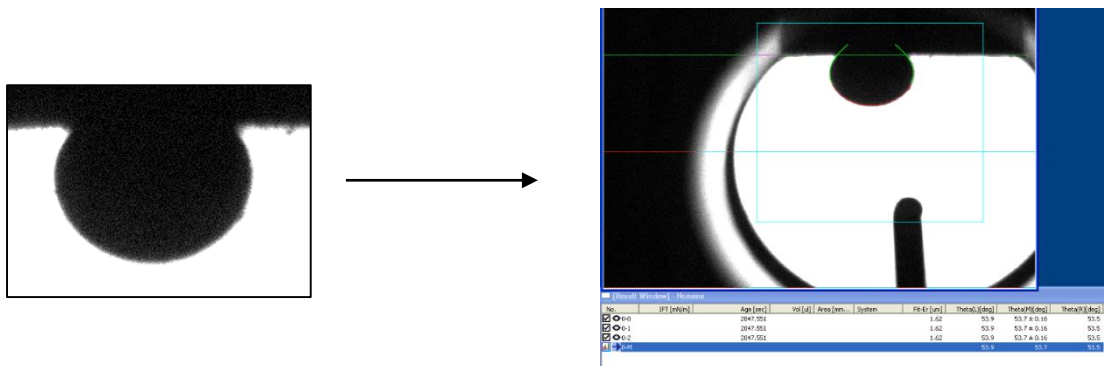


Fig. 4 — Analysis of the crude oil droplet

Contact Angle Experiments

This work consisted of two different studies. The effect of salinity on both waterflooding and water-alternating- CO_2 processes was evaluated for the Grey Berea system using three different brines: formation brine, seawater brine, and low-salinity brine (5,000 ppm NaCl). The effect of aging was evaluated through these experiments as well. The pressure of the system was maintained at 500 psi for all the cases. Through these experiments, the authors observed the effect of wettability alteration with the change in salinity of the brine.

An initial study was done to observe the effect of temperature on the contact angle of Grey Berea sandstone rock. This investigation used nitrogen as the pressurizing

medium. The temperature was varied between 77 °F and 176 °F at a constant interval of 9 °F, and the equilibrium contact angles were measured at each temperature.

Another study was conducted to observe the effect of CO₂ on the dynamic contact angle of Grey Berea sandstone rock. This study used CO₂ as the pressurizing medium. Dynamic contact angles were measured every 30 minutes for 24 hours. The temperature was set at 149 °F to simulate reservoir conditions.

Components of the Coreflood Apparatus

Fig. 5 shows a schematic diagram of the coreflood apparatus. It consisted of the following components:

1. A 20 in. stainless steel core holder. It contained a rubber sleeve that was used to apply overburden pressure on the core.
2. Three accumulators for oil, brine, and carbon dioxide.
3. An ISCO syringe pump that was used to inject the fluids into the core at constant flow rate.
4. A hydraulic pump that was used to apply overburden pressure on the core. It injected hydraulic oil into a cavity between the internal surface of the core holder and the rubber sleeve.
5. Regulators and gauges that monitored the pressure drop across the core over time.
6. A nitrogen cylinder that applied back pressure and overburden pressure and a carbon dioxide cylinder for WAG experiments.

7. A single pressure transducer that measured the pressure drop across the core. The pressure transducer was connected to LABVIEW software to record the pressure drop across the core versus time.
8. An electric oven which contained the coreholder. The core samples were placed inside the vertically mounted coreholder. The oven simulated reservoir temperature conditions for the core sample.

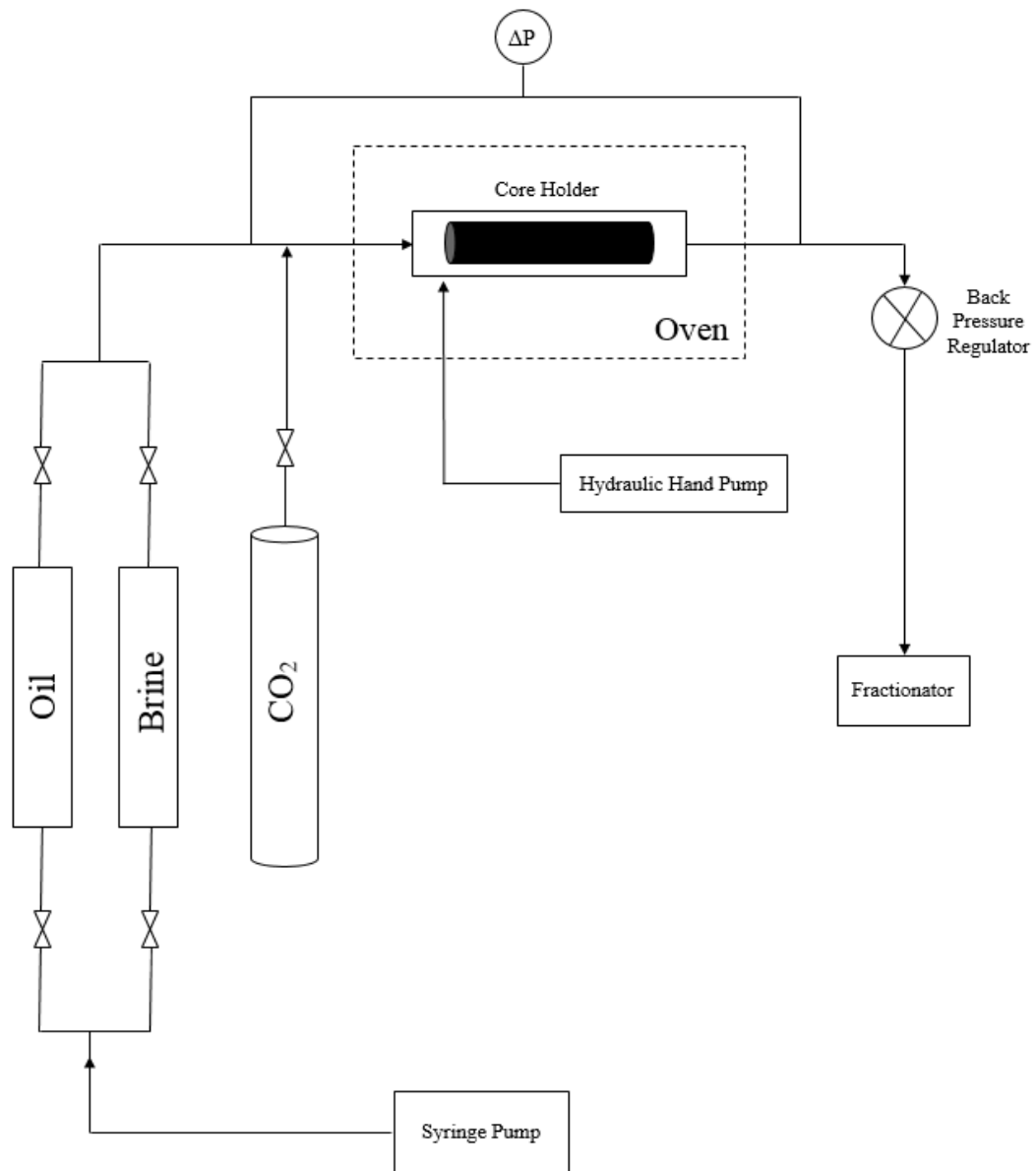


Fig. 5 — A schematic diagram of the coreflood apparatus.

Preparation of Cores

The procedure to prepare all the cores was the same. First, the 20 in. Grey Berea core was weighed before drying and the weight was noted. The core was then dried at 250 °F, and it was weighed every 24 hours until a constant weight was achieved. The core was then saturated with the synthetic formation brine in a saturation cell for at least 10 days to achieve ionic equilibrium between the core and the brine. A vacuum pump was used for four hours to remove the air pockets from the pores of each core. A coreflood system measured the brine saturation, the brine permeability, and the porosity of the core. The porosity of the core was calculated using the weight difference between the 100% brine saturated core and the dry core, divided by the density of formation brine. The permeability was measured at ambient conditions and using various injection rates of 0.5, 1, 1.5, 2, and 5 ml/min. The pressure drop across the core was constantly monitored and allowed to stabilize at a constant value to achieve a steady-state condition at a particular flow rate. This value of pressure drop was taken and the permeability was calculated using Darcy's equation. The backflow pressure and overburden pressure were kept at 500 psi and 1,000 psi, respectively.

Crude oil flooded the core to establish irreducible water saturation at different flow rates: 0.1, 0.2, 0.5, 1, 2, and 3 ml/min. Each flow rate was used until no connate water was produced from the core. The initial oil saturation and connate water saturation was calculated with the amount of produced brine at the end of the experiment. The back pressure and overburden were kept at 400 psi and 1,500 psi, respectively, for the oil flooding experiment. Aging was done for two of the six cores for a period of 30 days in a

sealed steel pipe filled with crude oil. It was done using an oven at a temperature of 149 °F. The pressure was kept at atmospheric condition.

Coreflood Experiments

This study involved six experiments using the Grey Berea sandstone samples. All of these experiments evaluated the performance of two types of recovery processes, i.e. waterflooding and water-alternating-CO₂ injection. The specific experiments included:

1. Low-salinity brine injection into an unaged core as a secondary mode of injection.
2. Seawater brine injection into an unaged core as a secondary mode of injection.
3. Low-salinity brine injection into an aged core as a secondary mode of injection.
4. Seawater brine injection into an aged core as a secondary mode of injection.
5. Low-salinity water-alternating-CO₂ injection into an unaged core as a secondary mode of injection.
6. Seawater-alternating-CO₂ injection into an unaged core as a secondary mode of injection.

The backflow pressure and the overburden pressure for all the experiments was kept at 500 psi and 1,500 psi, respectively. The temperature was maintained at 149 °F. These experiments were aimed to evaluate the effect of salinity of brine on the performance of waterflooding and water-alternating-CO₂. In this work, the secondary

recovery mode was initiated at initial oil saturation, S_{oi} . Different flow rates of injection were done to achieve residual oil saturation.

CHAPTER VII

RESULTS AND DISCUSSION

Effect of Salinity of Injected Brine on Contact Angle during Waterflooding Process

Wettability is affected by the salinity of the brine phase (Donaldson et al. 1969; Anderson 1986; Morrow 1990; Cuiec 1991; Morrow et al. 1998; Zhou et al. 2000; Chattopadhyay et al. 2002; Nasralla and Nasr-El-Din 2014). This study used three different brines with different salinities. These brines simulated a Middle East field at the same reservoir temperature condition. The temperature of the system affects the fluid-rock and fluid-fluid interactions, in turn changing the wettability of the rock. In this study, the contact angles of Grey Berea were measured at several temperatures, ranging from 77 °F to 176 °F. The system pressure was maintained at 500 psi for all the cases.

For unaged core substrates, the contact angles increased with temperature. When formation brine, seawater brine, or low-salinity brine was used as the brine phase in the Grey Berea-brine-nitrogen-oil system, the rock seemed to be water-wet for all temperatures. The contact angles increased from 42.5° to 59.5° in the case of formation brine for the temperature range. Similarly, the contact angles increased from 62.2° to 76.4° for seawater brine and 31.9° to 45° in the case of low-salinity brine for the temperature range.

Aged cores yielded higher contact angles for all the salinities. The contact angles increased from 64.7° to 78° in the case of formation brine for the temperature range. The contact angles ranged from 70° to 84° when seawater brine was used for the same temperature range. Similarly, the contact angles increased from 49.9° to 59.7° in the case

of low-salinity brine for the temperature range. As expected, aged cores had higher contact angles compared to the unaged cores (Zhou et al. 1996; Morrow et al. 1998; Chattopadhyay et al. 2002).

The graphical plots between the contact angle and temperature for unaged cores and aged cores are shown in **Fig. 6** and **Fig. 7**. The rock wettability was altered when low-salinity brine was used instead of the conventional formation brine to a more water-wet state. However, the rock became more oil-wet when seawater brine was used. This effect may be because of a bridging between the anionic surfactants of the crude oil and the increased number of divalent cations on the rock's surface. The addition of divalent cationic sites on the surface of the rock attracted the negative ends of polar components in crude oil (Buckley et al. 1998; Tang and Morrow 1999; Alotaibi et al. 2011). Monovalent cations, such as Na^+ , cover the rock's surface and prevent the interaction between the rock and crude oil. The ratio of divalent cations to monovalent cations in seawater brine is greater than formation brine, so the effect of bridging is more pronounced when seawater brine is used. As a result of the bridging, there is more interfacial energy between the rock and oil during seawater injection. The contact angle images for the Grey Berea-brine-oil-nitrogen system at 149°F is given in **Table 5**.

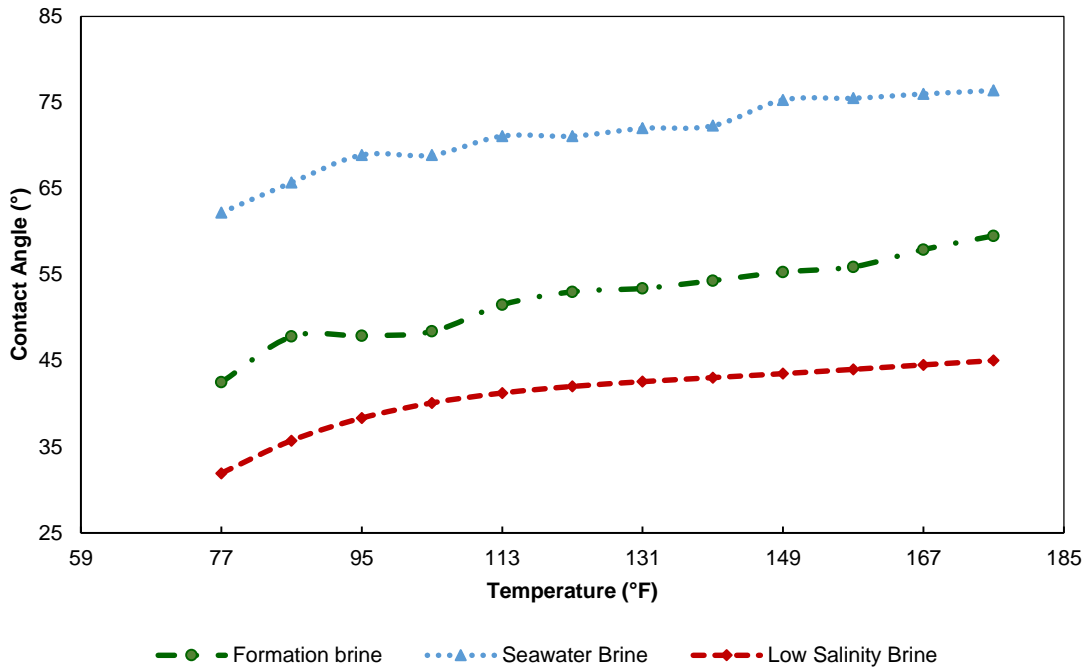


Fig. 6 — Effect of temperature on the equilibrium contact angle of unaged Grey Berea sandstone rock at 500 psi during waterflooding process.

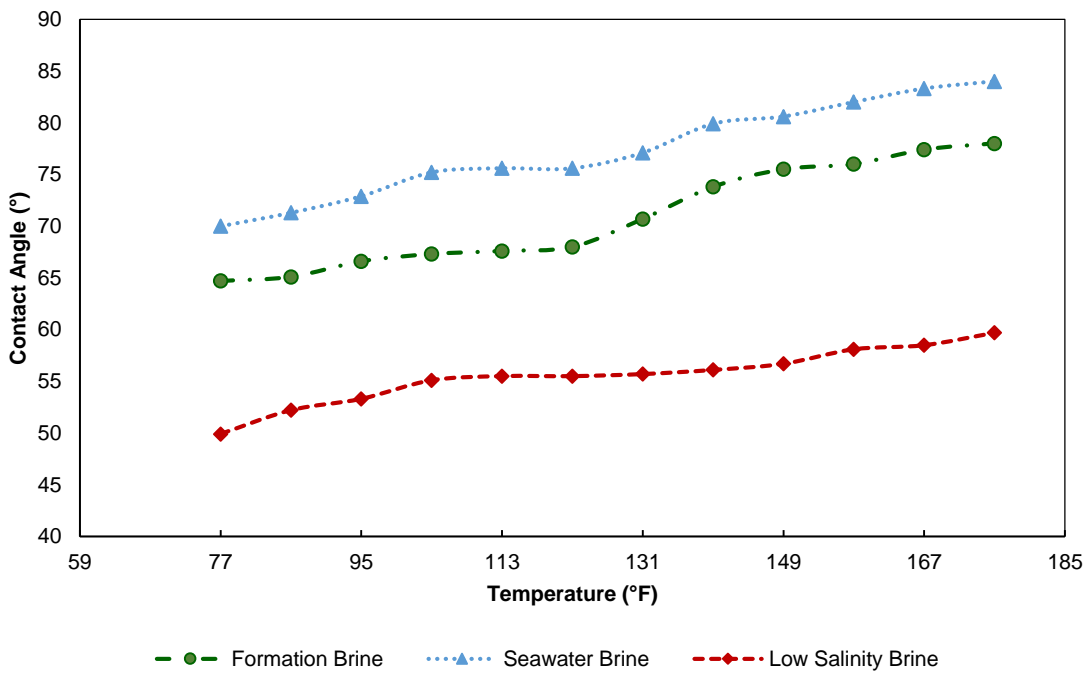


Fig. 3 — Effect of temperature on the equilibrium contact angle of aged Grey Berea sandstone rock at 500 psi during waterflooding process.

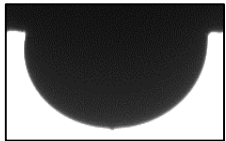
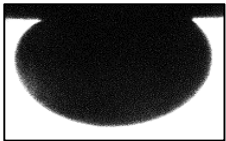
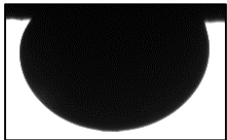
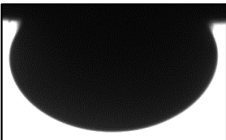
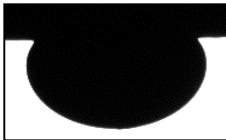
Aging Condition/Type of Brine	Formation Brine	Seawater Brine	Low-salinity Brine
Unaged	 $\theta = 55.3^\circ$	 $\theta = 75.3^\circ$	 $\theta = 43.5^\circ$
Aged	 $\theta = 75.5^\circ$	 $\theta = 80.6^\circ$	 $\theta = 56.7^\circ$

Table 5 — Equilibrium contact angle images of Grey Berea-brine-oil-nitrogen system at 149 °F.

Effect of Salinity of Injected Brine on Contact Angle during Water-Alternating-CO₂ Process

During a WAG process, the rock is exposed to three fluids: oil, brine and CO₂. The interactions between these phases can determine the wettability of the system. The change in salinity of the brine phase can alter the wettability of the rock. In this study, dynamic contact angles were measured for the Grey Berea-brine-oil-CO₂ system. The effect of salinity in this system was tested using three different brines. These brines simulated a Middle East field at the same reservoir temperature condition. Each study was done for 24 hours, and contact angle images were observed every 30 minutes.

For unaged core substrates, the dynamic contact angles fluctuated with time and reached a constant value after some time. Several factors including: penetration of crude oil into the rock, dissolution of CO₂ into the crude oil, light ends extraction, dissolution of micro drops of brine into oil, and strong electrostatic interactions between brine and crude

oil (Yang et al. 2008) resulted in the fluctuations in the contact angle. The system came into equilibrium when the effects counteracted against each other. For the formation brine case, the contact angles increased initially, then decreased, and increased again to become constant at 58° after 1,000 minutes of contact. The increase in contact angle can be attributed to the dissolution of CO_2 into the crude oil, and the decrease in contact angle can be attributed to light ends extraction from the crude oil, dissolution of micro drops of brine into oil, and strong electrostatic interactions between brine and crude oil. Similarly, in the case of seawater brine and low-salinity brine, the contact angles became constant around 75° after 1,320 minutes and 53.3° after 960 minutes. **Fig. 8** demonstrates the variation of contact angle with time for unaged cores.

The images of the equilibrium contact angle using different brines are given in **Table 6**. From the table, when low-salinity brine was used instead of formation brine, the rock became more water-wet as a result of reducing contact angles. Seawater brine showed more oil-wet conditions than formation brine. In all, low-salinity brine showed the lowest contact angles and most water-wetness amongst all of the three brines.

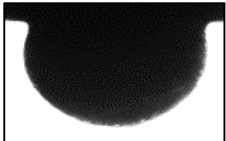
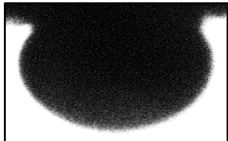
Aging Condition/Type of Brine	Formation Brine	Seawater Brine	Low-salinity Brine
Unaged	 $\theta = 58^\circ$	 $\theta = 75^\circ$	 $\theta = 53.3^\circ$

Table 6 — Equilibrium contact angle images of Grey Berea-brine-oil- CO_2 system at 149°F .

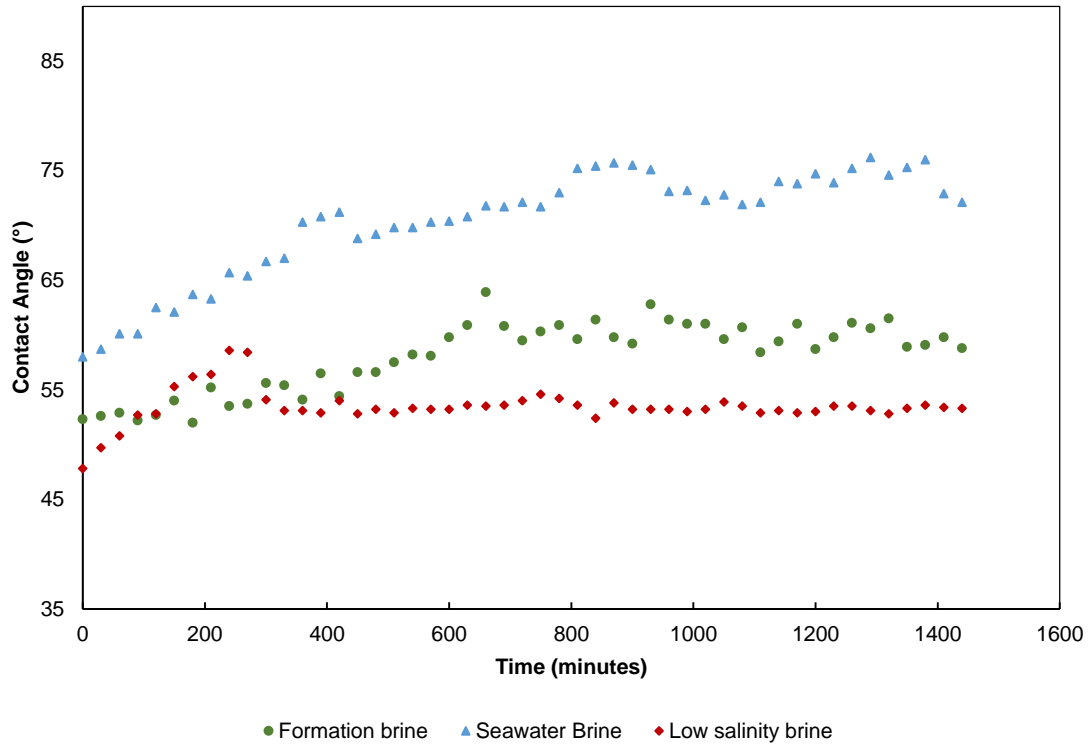


Figure 8 — Effect of time on the dynamic contact angle of unaged Grey Berea sandstone rock at 500 psi and 149 °F during water-alternating-CO₂ process.

Effect of Salinity of Injected Brine on Oil Recovery during Waterflooding

The effect of salinity of injected brine on oil recovery was studied using low-salinity brine and seawater brine as the injected brine. The authors performed four corefloods to test this effect. The cores for the experiments used the preparation procedure outlined in this paper.

Cores RSR 11, RSR 8, RSR 17, and RSR 5 were cut from the same block of outcrop Grey Berea. They had similar rock properties and similar fluid saturations. Low-salinity brine was flooded into RSR 11 and RSR 17 (Experiment A-1 and A-3, respectively), and RSR 8 and RSR 5 were flooded with seawater brine (Experiment A-2 and A-4, respectively). The experiments aimed at recovering oil as a secondary mode of recovery. A sealed steel pipe was used to age RSR 17 and RSR 8 for 30 days at 149 °F.

The experimental setup was similar for all the cores: Each core was mounted in a vertical coreholder and kept inside a high temperature oven. The temperature was set at 149 °F. The backflow pressure and overburden pressure was kept at 500 psi and 1,500 psi, respectively using nitrogen from the cylinder. After the temperature and pressure was set, the system was allowed to come into thermal equilibrium for at least two hours. The brine was kept in an accumulator outside the oven at standard atmospheric conditions. After the system achieved the target temperature, the brine was injected into the core using a Teledyne ISCO syringe pump. The injection process was done from the bottom of the core. Brine was injected at various flow rates: 0.5, 1, 2, and 4 ml/min. The number of pore volumes injected for each flow rate and the corresponding incremental oil recovery was measured and tabulated. The pressure drop between the ends of the core and oil recovered during the experiment are plotted.

Experiment A-1 led to an oil recovery of 22.74% OOIP with most of the oil recovered at 0.5 ml/min flow rate. 2.31% OOIP was recovered at 1 ml/min, and no oil recovery was observed at the later stages of injection. The oil production was high till water breakthrough. The pressure drop vs. time plot was stable and showed no signs of fines migration, precipitation, or plugging across the core. The jump in pressure drop signified the change of injection flow rate. **Fig. 9** shows the incremental oil recovery and pressure drop vs. time. **Table 7** presents the number of pore volumes injected for each slug.

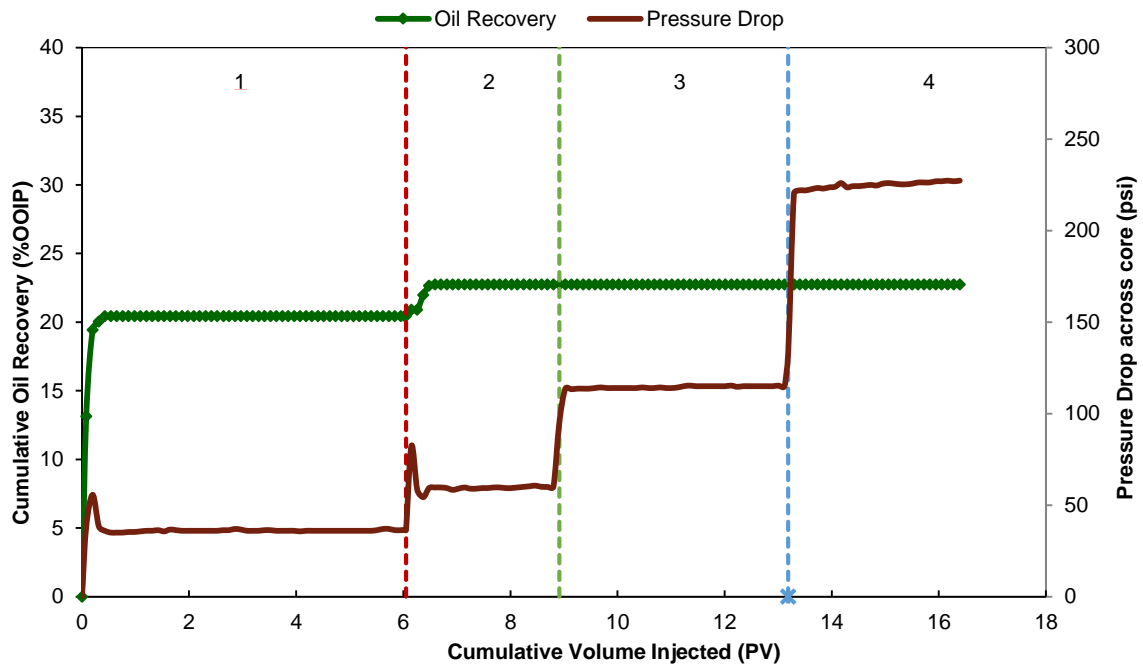


Fig. 9 — Oil recovery and pressure drop across the core for experiment A-1 at 149 °F. The injection was performed with NaCl brine (5,000 ppm) using injection rates of 0.5, 1, 2, and 4 ml/min. The vertical dashed lines separate the different injected brine stages.

Slug Type	Recovery Mode	Slug No.	Injection Rate (ml/min)	Slug Size (PV)	Incremental Oil Recovery (%OOIP)	Total Oil Recovery (%OOIP)
NaCl (5,000 ppm)	Secondary	1	0.5	6.051	20.43	20.43
		2	1	2.863	2.31	22.74
		3	2	4.273	0	22.74
		4	4	3.203	0	22.74

Table 7 — Summary of coreflood experiment (A-1) for unaged Grey Berea sandstone at T = 149 °F.

Experiment A-2 led to an oil recovery of 28.36% OOIP with 27.04% OOIP recovered at 0.5 ml/min. There was 1.14% OOIP recovered at 1 ml/min, and 0.18% OOIP recovered at 4 ml/min. There was no evidence of fines migration, precipitation, or plugging across the core. The jump in pressure drop signified the change of injection flow rate. **Fig. 10** shows the incremental oil recovery and pressure drop vs. time. **Table 8** presents the number of pore volumes injected for each slug.

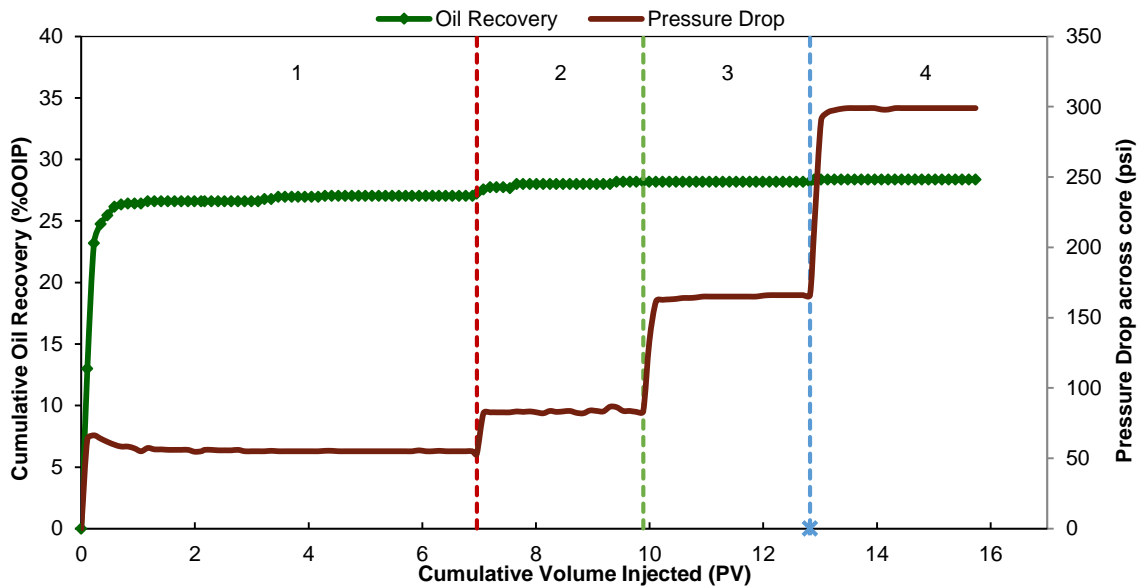


Fig. 40 — Oil recovery and pressure drop across the core for experiment A-2 at 149 °F. The injection was performed with seawater brine using injection rates of 0.5, 1, 2, and 4 ml/min. The vertical dashed lines separate the different injected brine stages.

Slug Type	Recovery Mode	Slug No.	Injection Rate (ml/min)	Slug Size (PV)	Incremental Oil Recovery (%OOIP)	Total Oil Recovery (%OOIP)
		1	0.5	6.96	27.04	27.04
Seawater Brine (54,680 ppm)	Secondary	2	1	2.93	1.14	28.18
		3	2	2.93	0	28.18
		4	4	2.91	0.18	28.36

Table 8 — Summary of coreflood experiment (A-2) for unaged Grey Berea sandstone at T = 149 °F.

From Fig. 6 and Fig. 7, experiment A-2 recovered 5.62% OOIP more than A-1. This increase in recovery is not considerable and may be attributed to a more oil-wet state of the rock when seawater brine is introduced into the system. From the contact angle measurements, one can confirm that from Table 5, the rock has a higher contact angle when seawater brine is introduced into the system compared to low-salinity brine. This increase in oil recovery during waterflooding due to wettability alteration towards a weakly water-wet system was observed by Jadhunandan and Morrow (1995).

From A-1, the authors can also conclude that low-salinity brine injection does not have an improved effect on oil recovery in unaged cores.

Experiment A-3 led to an oil recovery of 51.61% OOIP with most of the oil recovered at 0.5 ml/min flow rate. 1.46% OOIP was recovered at 1 ml/min, and no oil recovery was observed at later stages of injection. The oil production was high till water breakthrough and then decreased significantly. The pressure drop vs. time plot was stable and showed no signs of fines migration, precipitation, or plugging across the core. The jump in pressure drop signified the change of injection flow rate. **Fig. 11** shows the incremental oil recovery and pressure drop vs. time. **Table 9** presents the number of pore volumes injected for each slug.

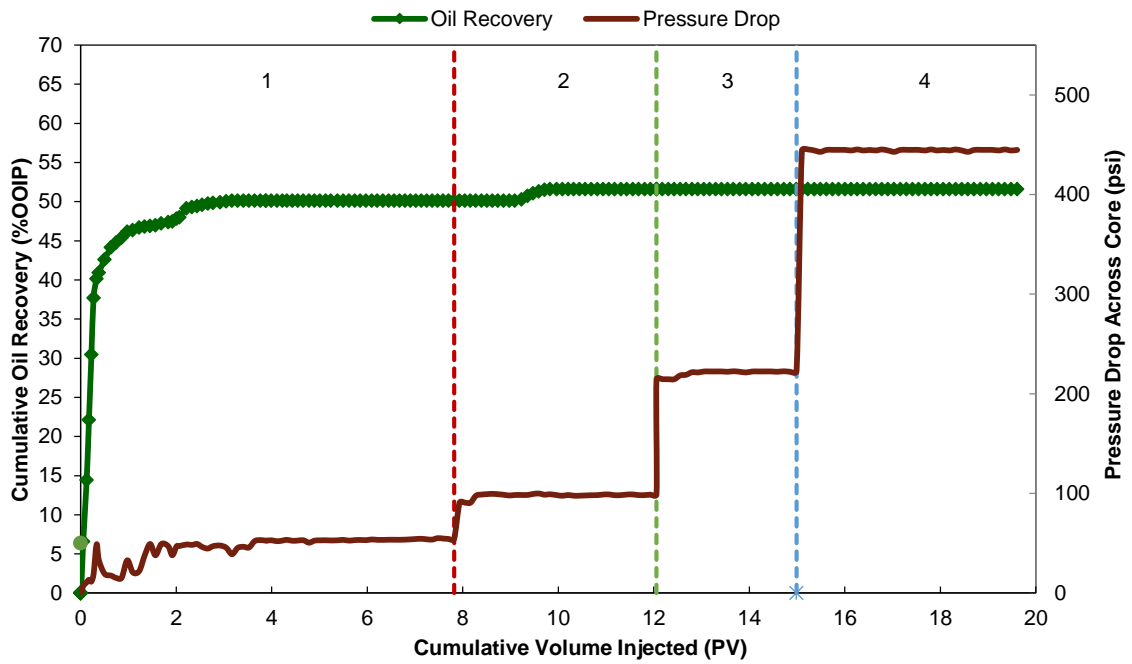


Fig. 51 — Oil recovery and pressure drop across the core for experiment A-3 at 149 °F. The injection was performed with NaCl brine (5,000 ppm) using injection rates of 0.5, 1, 2, and 4 ml/min. The vertical dashed lines separate the different injected brine stages.

Slug Type	Recovery Mode	Slug No.	Injection Rate (ml/min)	Slug Size (PV)	Incremental Oil Recovery (%OOIP)	Total Oil Recovery (%OOIP)
NaCl (5,000 ppm)	Secondary	1	0.5	7.82	50.15	50.15
		2	1	3.99	1.46	51.61
		3	2	3.17	0	51.61
		4	4	4.63	0	51.61

Table 9 — Summary of coreflood experiment (A-3) for aged Grey Berea sandstone at T = 149 °F.

Experiment A-4 led to an oil recovery of 32% OOIP, and there was no oil recovery in the remaining stages. There was no evidence of fines migration, precipitation, or plugging across the core. The jump in pressure drop signified the change of injection flow rate. **Fig. 12** shows the incremental oil recovery and pressure drop vs. time. Table 10 presents the number of pore volumes injected for each slug.

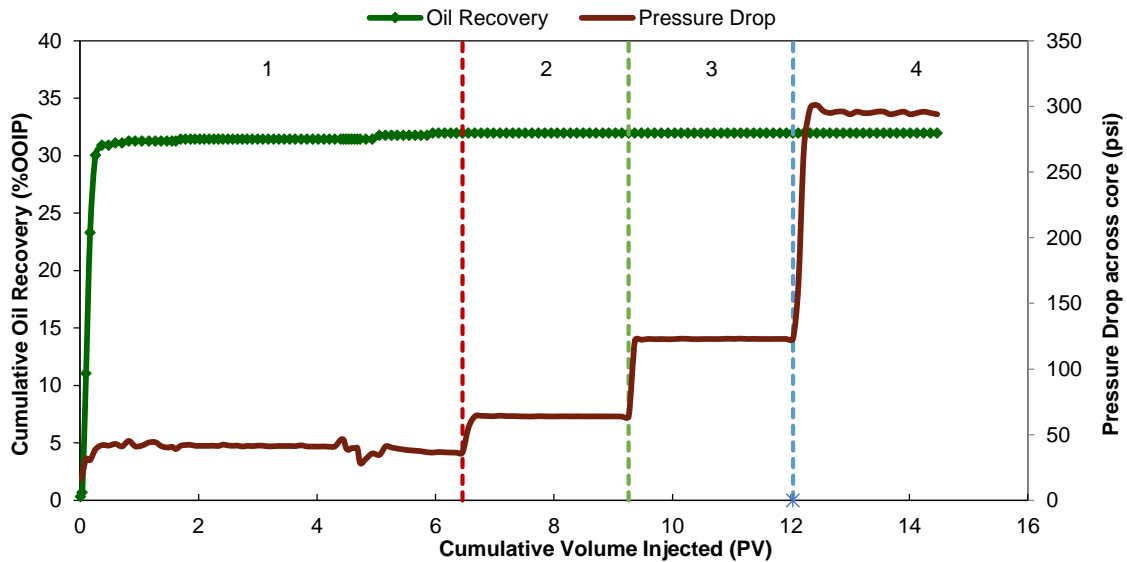


Fig. 62 — Oil recovery and pressure drop across the core for experiment A-4 at 149 °F. The injection was performed with seawater brine using injection rates of 0.5, 1, 2, and 4 ml/min. The vertical dashed lines separate the different injected brine stages.

Slug Type	Recovery Mode	Slug No.	Injection Rate (ml/min)	Slug Size (PV)	Incremental Oil Recovery (%OOIP)	Total Oil Recovery (%OOIP)
		1	0.5	6.46	32.0	32.0
Seawater Brine (54,680 ppm)	Secondary	2	1	2.802	0	32.0
		3	2	2.773	0	32.0
		4	4	2.434	0	32.0

Table 10 — Summary of coreflood experiment (A-4) for aged Grey Berea sandstone at T = 149 °F.

Experiment A-3 recovered 19.61% OOIP more than A-4. There was a definite case of wettability alteration towards a more water-wet state in this case. The contact angle when low-salinity brine was introduced was 56.7° while the contact angle when seawater brine was introduced was 80.6° , while all the remaining parameters remain constant. Clearly, when low-salinity brine was introduced into the system, the wettability of the rock changed and more oil was recovered.

Effect of Aging on Oil Recovery during Waterflooding

From Experiment A-1 and A-3, recovery improved when an aged core was used. 28.87% more oil was recovered during the low-salinity brine injection of an aged core. The aging of the core resulted in a more oil-wet condition of the rock, and this is shown in the contact angle measurements. The contact angle when an unaged core was used was 43.5° , while the contact angle when an aged core was used was 56.7° . Water-wetness decreased when an aged core was used instead of an unaged core. This could have resulted in the higher ultimate recovery of oil from the aged core (Zhou et al. 1996; Morrow et al. 1998; Chattopadhyay et al. 2002). Experiment A-2 and A-4 did not show much difference in the ultimate recovery of oil. There was a 3.64% OOIP more oil recovery in an aged core compared to the unaged core. Aging did not have a considerable effect on oil recovery during seawater brine injection.

Effect of Salinity of Injected Brine on Oil Recovery during WAG

Two corefloods demonstrated the effect of salinity of injected brine on oil recovery during WAG process. This study used unaged cores.

Cores RSR 20 and RSR 22 were cut from the same block of outcrop Grey Berea. They had similar rock properties and similar fluid saturations. RSR 20 was subjected to a low-salinity WAG flood (Experiment A-5), and RSR 22 was subjected to a seawater-brine-alternating-gas flood (Experiment A-6). Oil was recovered as a secondary mode of recovery.

The experimental setup for A-5 and A-6 were similar. The core was taken out from an oil accumulator and installed in a vertical coreholder. It was then kept inside a high temperature oven, and the temperature was set at 149 °F. The backflow pressure and overburden pressure was kept at 500 psi and 1,500 psi, respectively, using nitrogen from the cylinder. After the temperature and pressure was set, the system was allowed to come into thermal equilibrium for at least two hours. The brine was kept in an accumulator outside the oven at standard atmospheric conditions. The CO₂ was injected at 500 psi from a compressed CO₂ cylinder into a 1L accumulator for 20 minutes. A Teledyne syringe pump was used to maintain the pressure of CO₂ inside the accumulator to 500 psi. The syringe pump was used for at least 30 minutes before starting the experiment to achieve equilibrium. The scheme of injection was as follows:

Brine → CO₂ → Brine → CO₂ → Brine → CO₂

First, brine was injected at 0.5 ml/min from the bottom of the core. After the brine injection was over, CO₂ was injected at the same flow rate using the syringe pump. The injection was alternated with the help of valves. This cycle was repeated three times at different flow rates of 1, 2, and 4 ml/min. The number of pore volumes injected for each

slug and the corresponding incremental oil recovery was measured and tabulated. The pressure drop between the ends of the core and oil recovered during the experiment are plotted.

Experiment A-5 led to an oil recovery of 61.65% OOIP with 30.57% OOIP recovered during the first slug of low-salinity brine. The first slug of CO₂ recovered 12.84% OOIP; hence the first cycle of injection at 0.5 ml/min recovered 43.41% OOIP. The low-salinity brine in the second cycle at 1 ml/min recovered 4.73% OOIP, and the CO₂ slug recovered 1.52% OOIP. The second cycle at 2 ml/min recovered 6.25% OOIP in total. The third cycle of injection recovered 4.73% OOIP with low-salinity brine recovering 3.67% OOIP in the cycle. The fourth brine slug injection at 4 cc/min recovered 7.26% OOIP after 8.24 PV of injection. The process was stopped after the water cut became 100% for a long period of time. The process was stopped after this slug because of emulsion formation and discontinuity in pressure readings. **Fig. 13** shows the incremental oil recovery and pressure drop vs. time. **Table 11** presents the number of pore volumes injected for each slug.

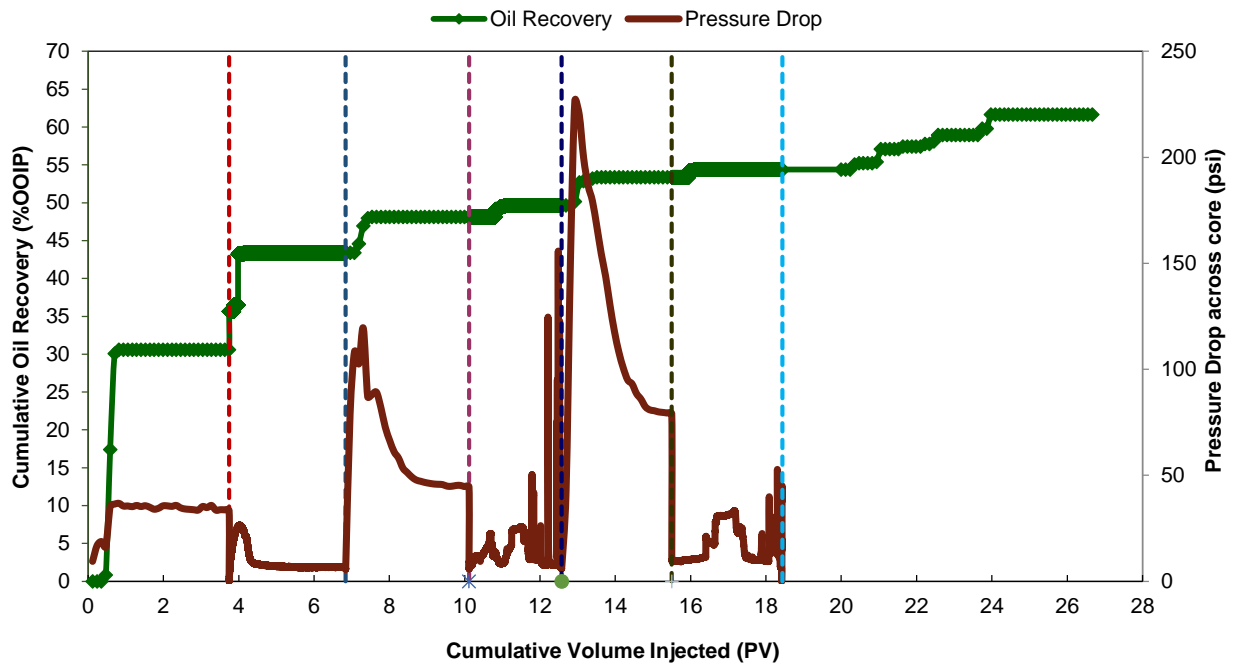


Fig. 73 — Oil recovery and pressure drop across the core for experiment A-5 at 149 °F. The injection was performed with low-salinity-brine-alternating-CO₂. The vertical dashed lines separate the different injection stages.

Slug No.	Slug Type	Recovery Mode	Injection Rate (ml/min)	Slug Size (PV)	Incremental Oil Recovery (%OOIP)	Total Oil Recovery (%OOIP)
1	NaCl (5,000 ppm)		0.5	3.74	30.57	30.57
2	CO ₂		0.5	3.1	12.84	43.41
3	NaCl (5,000 ppm)		1	3.28	4.73	48.14
4	CO ₂	Secondary	1	2.46	1.52	49.66
5	NaCl (5,000 ppm)		2	2.92	3.67	53.33
6	CO ₂		2	2.93	1.06	54.39
7	NaCl (5,000 ppm)		4	8.24	7.26	61.65

Table 11 — Summary of coreflood experiment (A-5) for unaged Grey Berea sandstone at T = 149 °F.

Continuous oil production occurred throughout the experiment because of gas finger diversion that contacts more oil in the core (Skauge and Sorbie 2014). The pressure drop vs. time plot showed a lot of peaks and troughs during the course of injection. The first cycle of injection showed stable graphs signifying no fines migration, precipitation, or plugging across the core. However, from the second cycle onwards, there were signs of peaks and troughs, mainly during CO₂ injection. This can be due to the displacement of oil within the core (Parracello et al. 2013), since oil was continuously produced throughout the experiment. The fluctuations may be also due to the increased solubility of CO₂ in brine (Zolfaghari et al. 2013).

The first slug of CO₂ produced a pressure drop lower than the first slug of brine injected. This is because of the lower viscosity of CO₂ as well as the greater relative permeability to CO₂. The brine injection during the second cycle at 1 ml/min produced a stable pressure drop that is lesser than double of the first cycle brine injection, even though the rate of injection was doubled. This trend was carried over to the remaining cycles as well. This is due to the reduced viscosity of oil and the increased relative permeability to water after the CO₂ slug (Aleidan and Mamora 2010). This may extrapolate to an increase in injectivity during field applications. The recovery was higher during the brine injection slugs than the gas injection slugs.

There was an indication of fines migration during the third and fourth cycle of injection. The authors observed oil-brine emulsions at high flow rates of 2 ml/min and 4 ml/min. The images of the emulsion formed are given in **Fig. 14**. Unfortunately, the

pressure drop during the fourth cycle of injection could not be recorded accurately due to blockage of the pressure transducer due to the emulsion.

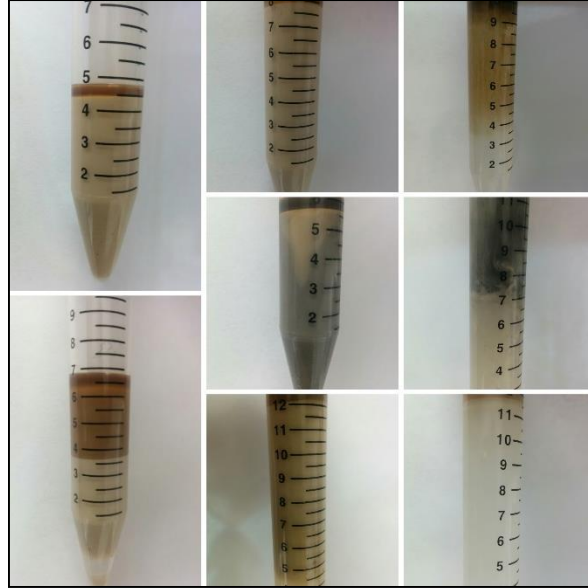


Fig. 14 — Emulsion formation as a result of fines migration in Experiment A-5.

Experiment A-6 recovered 64.58% OOIP with 37.83% OOIP recovered during the first slug of seawater brine injection at 0.5 ml/min. The first slug of CO₂ at 0.5 ml/min recovered only 0.63% OOIP. Hence, the total recovery during the first cycle of injection was 38.94% OOIP. The second cycle of injection recovered 11.55% OOIP with all the recovery obtained with seawater brine injection at 1 ml/min. The third slug of brine injected at 2 ml/min recovered 0.87% OOIP, and the third slug of CO₂ injected at 2 ml/min recovered 3.64% OOIP. The total oil recovered during the third cycle of injection was 4.51% OOIP. The fourth cycle of injection recovered 7.28% OOIP with seawater brine recovering 5.93% OOIP. A last slug of seawater brine was injected at 4 ml/min after the fourth cycle, and it recovered 2.3% OOIP. The injection was stopped after the water cut

became 100% for a long period of time. **Fig. 15** shows the incremental oil recovery and pressure drop vs. time. **Table 12** presents the number of pore volumes injected for each slug.

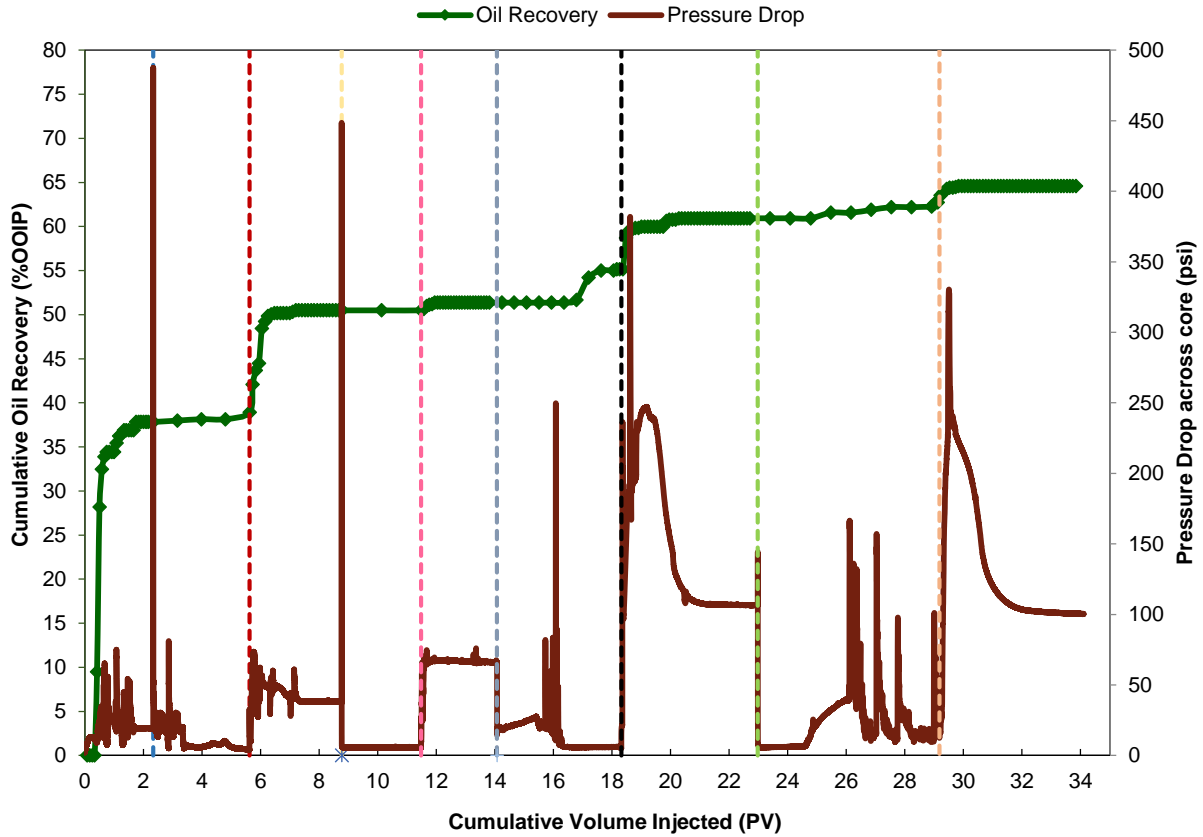


Figure 15 — Oil recovery and pressure drop across the core for experiment A-6 at 149 °F. The injection was performed with seawater-brine-alternating-CO₂. The vertical dashed lines separate the different injection stages.

Slug No.	Slug Type	Recovery Mode	Injection Rate (ml/min)	Slug Size (PV)	Incremental Oil Recovery (%OOIP)	Total Oil Recovery (%OOIP)
1	Seawater Brine (54,680 ppm)		0.5	2.34	37.83	37.83
2	CO ₂		0.5	3.29	1.11	38.94
3	Seawater Brine (54,680 ppm)		1	3.15	11.55	50.49
4	CO ₂		1	2.71	0	50.49
5	Seawater Brine (54,680 ppm)	Secondary	2	2.59	0.87	51.36
6	CO ₂		2	4.24	3.64	55.00
7	Seawater Brine (54,680 ppm)		4	4.65	5.93	60.93
8	CO ₂		4	6.20	1.35	62.28
9	Seawater Brine (54,680 ppm)		4	4.93	2.3	64.58

Table 12 — Summary of coreflood experiment (A-6) for unaged Grey Berea sandstone at T = 149 °F.

There was continuous oil production throughout the experiment because of gas finger diversion that contacts more oil in the core (Skauge and Sorbie 2014). The pressure drop vs time plot showed similar response to A-5. The displacement of oil in the core caused many troughs and peaks. The oil viscosity was reduced, and the relative permeability to water increased. However, there was no indication of fines migration in this experiment. The recovery was higher during the brine injection slugs than that with the gas injection slugs.

Comparing experiments A-5 and A-6, 2.93% more oil recovery resulted during seawater brine WAG. Although this is not substantial, one can say that the increase in

recovery may be due to the lower solubility of CO₂ in seawater brine compared to low-salinity brine (Jiang et al. 2010). This allows more CO₂ to contact the oil and reduce its viscosity. Also, during seawater brine WAG, the rock tends to be more mixed-wet compared to the rock's water-wet condition during low-salinity WAG. This can be confirmed using the contact angle measurements, as shown in Table 6. Huang and Holm (1988) also pointed out that there is a large amount of oil trapping during CO₂ WAG in preferentially water-wet cores.

Waterflooding vs. WAG

Both the WAG experiments (A-5 and A-6) recovered significantly more oil than its counterpart waterflooding process (A-1 and A-2). Low-salinity WAG recovered 37.73% OOIP more than low-salinity brine injection, and seawater WAG recovered 36.22% OOIP more than seawater brine injection. The reason for this can be attributed to the decrease in oil viscosity due to CO₂, trapped gas saturation (Holmgren and Morse 1951; Skauge 1996), gas diversion (Skauge and Sorbie 2014), and low pH buffer solution developed by CO₂ (Zolfaghari et al. 2013). **Fig. 16** compares the oil recovered during all the coreflood experiments performed in this paper.

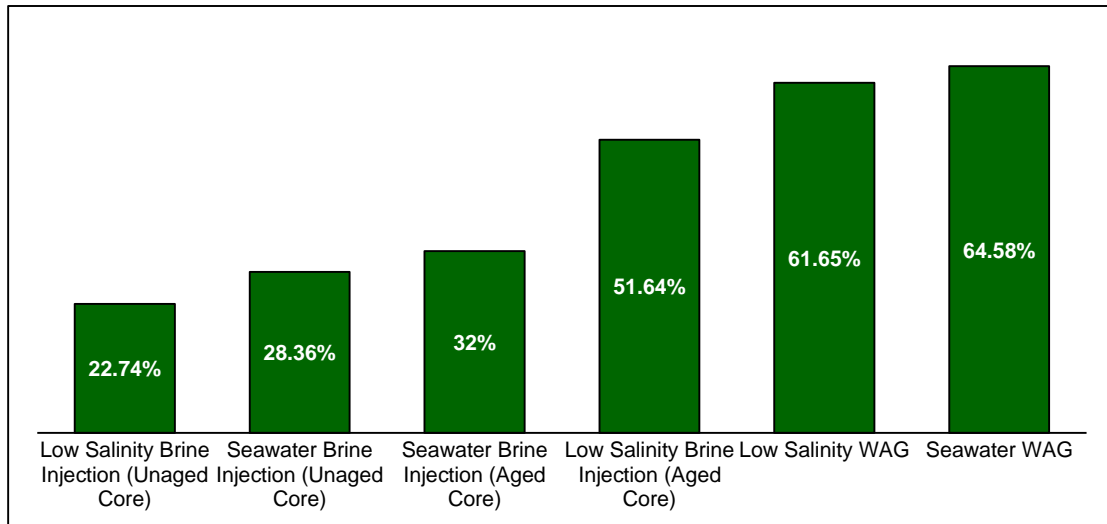


Fig. 16 — Comparison of oil recovery between different processes on Grey Berea sandstone at T = 149°F.

CHAPTER VIII

CONCLUSIONS

Results of this research led to the following conclusions:

1. The salinity of injected brine was a very important factor in the overall recovery of oil for both stand-alone brine injection and water-alternating-CO₂ injection. Seawater brine gave higher ultimate recovery in both waterflooding and WAG processes for unaged cores.
2. The aging of the cores played a very important role in the recovery of oil. There was more oil recovered after aging the cores. Also, low-salinity brine injection recovered more oil than seawater brine with aged cores.
3. In general, water-alternating-CO₂ injection produced more oil than a waterflooding process. CO₂ reduced the viscosity of the oil and lowered the pH environment by creating a buffer. Also, gas diversion and trapped gas saturation helped to recover more oil.
4. Fines migration was observed during low-salinity WAG with the formation of emulsions. This may be due to the presence of kaolinite in the cores.
5. The salinity of injected brine proved significant in changing the wettability of the rock. Low-salinity brines produced the lowest contact angles.
6. Contact angle measurements proved that aged cores had higher contact angles than unaged cores. Brines with divalent ions allowed the oil to be adsorbed to the surface of the rock via ion binding to produce more oil-wet states.

7. This research will contribute to the understanding of the effect of salinity of injected brine during waterflooding and water-alternating-CO₂ injection processes. It will also show the effect of salinity of injected brine on the wettability of the rock during these processes. This work could lead to the optimization of the salinity of injected brine and, hence, a better recovery factor and project economics.

REFERENCES

- Agbalaka, C., Dandekar, A.Y., Patil, S. et al. 2008. The Effect of Wettability on Oil Recovery: A Review. Presented at the SPE Asia Pacific Oil and Gas Conference and Exhibition, Perth, Australia, 20–22 October. SPE-114496-MS. <http://dx.doi.org/doi:10.2118/114496-MS>.
- Aleidan, A. and Mamora, D.D. 2010. SWACO₂ and WACO₂ Efficiency Improvement in Carbonate Cores by Lowering Water Salinity. Presented at the Canadian Unconventional Resources and International Petroleum Conference, Calgary, 19–21 October. SPE-137548-MS. <http://dx.doi.org/10.2118/137548-MS>.
- Al-Netaifi, A.S. 2008. Experimental Investigation of CO₂ – Miscible Oil Recovery at Different Conditions. MS thesis, King Saud University, Riyadh, Saudi Arabia.
- Ali, H.A.A.A and Schechter, D.S. 2013. Application of Polymer Gels as Conformance Control Agents for Carbon Dioxide EOR WAG Floods. Presented at the 2013 SPE International Symposium on Oilfield Chemistry, The Woodlands, TX, 8–10 April. SPE-164096-MS. <http://dx.doi.org/10.2118/164096-MS>.
- Alotaibi, M.B., Nasralla, R.A., and Nasr-El-Din, H.A. 2011. Wettability Studies Using Low-Salinity Water in Sandstone Reservoirs. *SPE Res Eval & Eng* **14** (6): 713–725. <http://dx.doi.org/10.2118/149942-PA>.
- Alvarado, V. and Manrique, E. 2010. Enhanced Oil Recovery: An Update Review. *Energies* **3**(9), 1529–1575.
- Ameri, A., Kaveh, N.S., Rudolph, E.S.J., Wolf, K-H. et al. 2013. Investigation on Interfacial Interactions among Crude Oil – Brine – Sandstone Rock – CO₂ by Contact Angle Measurements. *Energy Fuels* **27**: 1,015–1,025. <http://dx.doi.org/10.1021/ef3017915>.
- Anderson, W.G. 1986. Wettability Literature Survey – Part 2: Wettability Measurements. *J Pet Technol* **38** (11): 1,246–1,262. SPE-13933-PA. <http://dx.doi.org/10.2118/13933-PA>.
- Beeson, D.M. and Ortloff, G.D. 1959. Laboratory Investigation of the Water-Driven Carbon Dioxide Process for Oil Recovery. *J Pet Technol* **11** (4): 63–66.
- Buckley, J.S., Takamura, K., and Morrow, N.R. 1989. Influence of Electrical Surface Charges on the Wetting Properties of Crude Oils. *SPE Res Eng* **4** (3): 332–340.
- Buckley, J.S., Liu, Y., and Monsterleet, S. 1998. Mechanisms of Wetting Alteration by Crude Oils. *SPE J.* **3** (1): 54–61. <http://dx.doi.org/doi:10.2118/37230-PA>.

- Caudle, B.H. and Dyes, A.B. 1958. Improving Miscible Displacement by Gas-Water Injection. *Trans. AIME* **213**: 281–284.
- Chattopadhyay, S., Jain, V., and Sharma, M.M. 2002. Effect of Capillary Pressure, Salinity, and Aging on Wettability Alteration in Sandstones and Limestones. Presented at the SPE/DOE Improved Oil Recovery Symposium, Tulsa, OK, 13–17 April. SPE-75189-MS. <http://dx.doi.org/doi:10.2118/75189-MS>.
- Chen, S., Li, H., Yang, D. et al. 2010. Optimal Parametric Design for Water-Alternating-Gas (WAG) Process in a CO₂-Miscible Flooding Reservoir. *J Can Pet Technol* **49** (10): 75–82. <http://dx.doi.org/doi:10.2118/141650-PA>.
- Cuiec, L.E. 1991. Evaluation of Reservoir Wettability and its Effect on Oil Recovery. *Interfacial Phenomena in Petroleum Recovery*. Edition Morrow, N.R. Marcel Dekker, Inc., New York and Basel.
- Dang, C.T., Nghiem, L.X., Chen, Z. et al. 2013. State-of-the-Art Low Salinity Waterflooding for Enhanced Oil Recovery. Presented at the SPE Asia Pacific Oil and Gas Conference and Exhibition, Jakarta, Indonesia, 22–24 October. SPE-75189-MS. <http://dx.doi.org/10.2118/75189-MS>.
- Dang, C.T.Q., Nghiem, L.X., and Chen, Z. 2014. CO₂ Low Salinity Water Alternating Gas : A New Promising Approach for Enhanced Oil Recovery. Presented at the SPE Improved Oil Recovery Symposium, Tulsa, OK, 12–16 April. SPE-169071-MS. <http://dx.doi.org/10.2118/169071-MS>.
- Dong, M., Huang, S., and Srivastava, R. 2000. Effect of Solution Gas in Oil on CO₂ Minimum Miscibility Pressure. *J Can Pet Technol* **39** (11). <http://dx.doi.org/doi:10.2118/00-11-05>.
- Donaldson, E.C., Thomas, R.D., and Lorenz, P.B. 1969. Wettability Determination and Its Effect on Recovery Efficiency. *SPE J.* **9** (1). SPE-2338-PA. <http://dx.doi.org/10.2118/2338-PA>.
- Enick, R.M., Olsen, D., Ammer, J.W. et al. 2012. Mobility and Conformance Control for CO₂ EOR via Thickeners, Foams, and Gels —A Literature Review of 40 Years of Research and Pilot Tests. Presented at the Eighteenth SPE Improved Oil Recovery Symposium, Tulsa, OK, 14–18 April. SPE-154122-MS. <http://dx.doi.org/doi:10.2118/154122-MS>.
- Ghedan, S. 2009. Global Laboratory Experience of CO₂-EOR Flooding. Presented at the 2009 SPE/EAGE Reservoir Characterization and Simulation Conference, Abu Dhabi, UAE, 19–21 October. SPE-125581-MS. <http://dx.doi.org/10.2118/125581-MS>.

- Graue, D.J. and Zana, E.T. 1981. Study of a Possible CO₂ Flood in Rangely Field. *J Pet Technol*, **33** (7): 1–312.
- Hild, G.P. and Wackowski, R.K. 1999. Reservoir Polymer Gel Treatments to Improve Miscible CO₂ Flood. *SPE Res Eval & Eng* **2** (2): 19–22.
<http://dx.doi.org/doi:10.2118/56008-PA>.
- Holm, L.W. 1959. Carbon Dioxide Solvent Flooding for Increased Oil Recovery. *Trans. AIME* **216**: 225–231.
- Holm, W. 1987. Evolution of the Carbon Dioxide Flooding Processes. *J Pet Technol* **39** (11): 1,337–1,342. <http://dx.doi.org/doi:10.2118/17134-PA>.
- Holmgren, C.R. and Morse, R.A. 1951. Effect of Free Gas Saturation on Oil Recovery by Water Flooding. *J Pet Technol* **3** (5): 135–140.
<http://dx.doi.org/doi:10.2118/951135-G>.
- Huang, E.T.S. and Holm, L.W. 1988. Effect of WAG Injection and Rock Wettability on Oil Recovery during CO₂ Flooding. *SPE Res Eng* **3** (1): 119–129.
<http://dx.doi.org/doi:10.2118/15491-PA>.
- Jadhunandan, P. 1990. Effects of Brine Composition, Crude Oil and Aging Conditions on Wettability and Oil Recovery. PhD dissertation, New Mexico Institute of Mining and Technology, Socorro.
- Jadhunandan, P.P. and Morrow, N.R. 1995. Effect of Wettability on Waterflood Recovery for Crude-Oil/Brine/Rock Systems. *SPE Res Eng* **10** (1): 40–46.
<http://dx.doi.org/doi:10.2118/22597-PA>.
- Jaeger, P.T., Alotaibi, M.B., and Nasr-El-Din, H.A. 2010. Influence of Compressed Carbon Dioxide on the Capillarity of the Gas - Crude Oil - Reservoir Water System. *Journal of Chemical & Engineering Data* **55** (11): 5,246–5,251.
- Jiang, H., Nuryaningsih, L., and Adidharma, H. 2010. The Effect of Salinity of Injection Brine on Water Alternating Gas Performance in Tertiary Miscible Carbon Dioxide Flooding : Experimental Study. Presented at SPE Western Regional Meeting, Anaheim, California, 27–29 May. SPE-132369-MS.
<http://dx.doi.org/10.2118/132369-MS>.
- Johnson, W. E., Macfarlane, R. M., Breston, J. N. et al. 1952. Laboratory Experiments with Carbonated Water and Liquid Carbon Dioxide as Oil Recovery Agents. *Prod. Monthly* **17** (1): 15.

- Kamali, F., Hussain, F., and Cinar, Y. 2015. A Laboratory and Numerical-Simulation Study of Co-Optimizing CO₂ Storage and CO₂ Enhanced Oil Recovery. *SPE J.* SPE-171520-PA (in press; posted June 2015).
- Kulkarni, M.M. and Rao, D.N. 2005. Experimental investigation of miscible and immiscible Water-Alternating-Gas (WAG) process performance. *Journal of Petroleum Science and Engineering* **48** (1): 1–20. <http://dx.doi.org/doi:10.1016/j.petrol.2005.05.001>
- Lager, A., Webb, K. J., Black, C. J. J. et al. 2008. Low Salinity Oil Recovery-An Experimental Investigation. *Petrophysics* **49** (1).
- Ligthelm, D.J., Gronsveld, J.P., Hofman, N.J. et al. 2009. Novel Waterflooding Strategy by Manipulation of Injection Brine Composition. Presented at EUROPEC/EAGE Conference and Exhibition, Amsterdam, The Netherlands, 8–11 June, SPE-119835-MS. <http://dx.doi.org/10.2118/119835-MS>.
- Manrique, E.J., Muci, V.E., and Gurfinkel, M.E. 2007. EOR Field Experiences in Carbonate Reservoirs in the United States. *SPE Res Eval & Eng* **10** (6): 667–686.
- Martin, D. and Taber, J.J. 1992. Carbon Dioxide Flooding. *J Pet Technol* **44** (4): 396–400. <http://dx.doi.org/doi:10.2118/23564-PA>.
- McClain, J.B., Betts, D.E., Canelas, D.A. et al. 1996. Characterization of Polymers and Amphiphiles in Supercritical CO₂ using Small Angle Neutron Scattering and Viscometry. Presented at the Spring Meeting of the ACS, Division of Polymeric Materials, Vol. 74, 234–235. New Orleans, LA.
- McGuire, P.L., Chatham, J.R., Paskvan, F.K. et al. 2005. Low Salinity Oil Recovery: An Exciting New EOR Opportunity for Alaska’s North Slope. Presented at the SPE Western Regional Meeting, Irvine, California, USA, 30 March–1 April. SPE-93903-MS. <http://dx.doi.org/10.2118/93903-MS>.
- Morrow, N. 1990. Wettability and Its Effect on Oil Recovery. *J Pet Technol* **42** (12): 1,476–1,484. <http://dx.doi.org/doi:10.2118/21621-PA>.
- Morrow, N.R., Tang, G.Q., Valat, M. et al. 1998. Prospects of Improved Oil Recovery Related to Wettability and Brine Composition. *Journal of Petroleum Science and Engineering* **20** (3): 267–276.
- Nasralla, R.A., Bataweel, M.A., and Nasr-El-Din, H.A. 2013. Investigation of Wettability Alteration and Oil-Recovery Improvement by Low-Salinity Water in Sandstone Rock. *J Can Pet Technol* **52** (2): 144–154. <http://dx.doi.org/doi:10.2118/146322-PA>.

- Nasralla, R.A. and Nasr-El-Din, H.A. 2014. Double-Layer Expansion: Is It a Primary Mechanism of Improved Oil Recovery by Low-Salinity Waterflooding? *SPE Res Eval & Eng* **17** (1): 49–59. SPE-154334-PA. <http://dx.doi.org/10.2118/154334-PA>.
- Orr Jr., F.M., Silva, M.K., Lien, C.L. et al. 1982. Laboratory Experiments to Evaluate Field Prospects for CO₂ Flooding. *J Pet Technol* **34** (4): 888–898. <http://dx.doi.org/doi:10.2118/9534-PA>.
- Parracello, V.P., Bartosek, M., and Masserano, F. 2013. Experimental Investigation of Immiscible Water Alternating Gas (WAG) in Viscous Oil. Presented at the Offshore Mediterranean Conference and Exhibition, Ravenna, Italy, 20–22 March. OMC-2013-093.
- Sahin, S., Kalfa, U., and Celebioglu, D. 2012. Unique CO₂ - Injection Experience in the Bati Raman Field May Lead to a Proposal of EOR / Sequestration CO₂ Network in the Middle East. *SPE Econ & Mgmt* **4** (1): 42–50. SPE-139616-PA. <http://dx.doi.org/10.2118/139616-PA>.
- Shehata, A.M. and Nasr-El-Din, H.A. 2015. Zeta Potential Measurements : Impact of Salinity on Sandstone Minerals. Presented at the SPE International Symposium on Oilfield Chemistry, The Woodlands, Texas, 13–15 April. SPE-173763-MS. <http://dx.doi.org/10.2118/173763-MS>.
- Sinisha, J. 2012. CO₂ EOR : Nanotechnology for Mobility Control Studied. *J Pet Technol* **64** (7): 28–31. SPE-0712-0028-JPT. <http://dx.doi.org/10.2118/0712-0028-JPT>.
- Skauge, A. 1996. Influence of Wettability on Trapped Non-Wetting Phase Saturation in Three-Phase Flow. Proceeding Fourth International Symposium on Wettability and its Effect on Oil Recovery, 11–13 September, Montpellier, France.
- Skauge, A. and Sorbie, K. 2014. Status of Fluid Flow Mechanisms for Miscible and Immiscible WAG. Presented at the SPE EOR Conference at Oil and Gas West Asia, Muscat, Oman, 31 March–2 April. SPE-169747-MS. <http://dx.doi.org/10.2118/169747-MS>.
- Sohrabi, M., Mahzari, P., Farzaneh, S.A. et al. 2015. Novel Insights into Mechanisms of Oil Recovery by Low Salinity Water. Presented at the SPE Middle East Oil & Gas Show and Conference, Manama, Bahrain, 8–11 March. SPE-172778-MS. <http://dx.doi.org/10.2118/172778-MS>.
- Stalkup, F.I. 1978. Carbon Dioxide Miscible Flooding: Past, Present, and Outlook for the Future. *J Pet Technol* **30** (8): 1–102. <http://dx.doi.org/doi:10.2118/7042-PA>.

- Tang, G.Q. and Morrow, N.R. 1999. Influence of Brine Composition and Fines Migration on Crude Oil/brine/rock Interactions and Oil Recovery. *Journal of Petroleum Science and Engineering* **24** (2): 99–111.
- Thomas, G.A. and Monger-McClure, T.G. 1991. Feasibility of Cyclic CO₂ Injection for Light-Oil Recovery. *SPE Res Eng* **6** (2): 179–184. <http://dx.doi.org/doi:10.2118/20208-PA>.
- Wang, W. and Gupta, A. 1995. Investigation of the Effect of Temperature and Pressure on Wettability Using Modified Pendant Drop Method. Presented at the SPE Annual Technical Conference and Exhibition, Dallas, Texas, 22–25 October. SPE-30544-MS. <http://dx.doi.org/doi:10.2118/30544-MS>.
- Webb, K.J., Black, C.J.J., and Al-Ajeel, H. 2004. Low Salinity Oil Recovery - Log-Inject-Log. Presented at the SPE/DOE Symposium on Improved Oil Recovery, Tulsa, OK, 7–21 April. SPE-89379-MS. <http://dx.doi.org/10.2118/89379-MS>.
- Woods, P., Schramko, K., Turner, D. et al. 1986. In-Situ Polymerization Controls CO₂/Water Channeling at Lick Creek. Paper presented at the SPE Enhanced Oil Recovery Symposium, Tulsa, Oklahoma, 20–23 April. SPE-14958-MS. <http://dx.doi.org/10.2118/14958-MS>.
- Yang, D., Gu, Y., and Tontiwachwuthikul, P. 2008. Wettability Determination of the Crude Oil–Reservoir Brine–Reservoir Rock System with Dissolution of CO₂ at High Pressures and Elevated Temperatures. *Energy & Fuels* **22** (4): 2,362–2,371.
- Yildiz, H. O., Valat, M., and Morrow, N.R. 1999. Effect of Brine Composition on Wettability and Oil Recovery of a Prudhoe Bay Crude Oil. *J Can Pet Technol* **38** (1): 26–31. <http://dx.doi.org/doi:10.2118/99-01-02>.
- Zhou, X., Morrow, N.R., and Ma, S. 1996. Interrelationship of Wettability, Initial Water Saturation, Aging Time and Oil Recovery by Spontaneous Imbibition and Waterflooding. Presented at the SPE/DOE 10th symposium on Improved Oil Recovery, Tulsa, OK, April 1996, SPE-35436-PA. <http://dx.doi.org/10.2118/62507-PA>.
- Zhou, X., Morrow, N., and Ma, S. 2000. Interrelationship of Wettability, Initial Water Saturation, Aging Time, and Oil Recovery by Spontaneous Imbibition and Waterflooding. *SPE J.* **5** (2): 21–24. <http://dx.doi.org/doi:10.2118/62507-PA>.
- Zolfaghari, H., Zebarjadi, A., Shahrokhi, O. et al. 2013. An Experimental Study of CO₂ - Low Salinity Water Alternating Gas Injection in Sandstone Heavy Oil Reservoirs. *Iranian Journal of Oil & Gas Science & Technology* **2** (3): 37–47.